An Artificial Intelligence Method for Energy Efficient Operation of Blast Furnace in Steel Making Industry

By

Muhammad Salman Arif

School of Chemical and Materials Engineering

National University of Sciences and Technology

2021

An Artificial Intelligence Method for Energy Efficient Operation of Blast Furnace in Steel Making Industry

Muhammad Salman Arif

2018-MS PSE-01-00000276298

This work is submitted as a MS thesis in partial fulfillment of the requirement for the degree of

MS in Process Systems Engineering

Supervisor Name: Dr. Iftikhar Ahmad

School of Chemical and Materials Engineering (SCME)

National University of Sciences and Technology (NUST)

H-12 Islamabad, Pakistan

August, 2021

Dedication

"This thesis is dedicated to family, teachers and friends for endless *motivation, support and encouragement throughout the research"*

Abstract

The iron melting furnaces are the most energy-consuming equipment of the iron and steel industry. The energy efficiency of the furnace is affected by process conditions such as the inlet temperature, velocity of the charge, and composition of the charge. Hence, optimum values of these process conditions are vital in the efficient operation of the furnace. Computational methods have been very helpful in the optimum design and operation of process equipment. In this study, a first principle (FP) model was developed for an iron-making furnace to visualize its internal dynamics. To minimize the large computational time required for the FP-based analysis, a data-based model, i.e., Artificial Neural Networks (ANN), is developed using data extracted from the FP model. The ANN model was developed using data sets comprised of the values of temperature of the charge and gasses, velocity, concentration of the oxygen, pressure, airflow directions, energy and exergy profiles, and overall exergy efficiency of the furnace along with its height. The ANN model was highly accurate in prediction and is suitable for real-time implementation in a steel manufacturing plant.

Keywords: Blast Furnace; MATLAB; physical exergy; Artificial Neural network.

.

Acknowledgments

All thanks to **Almighty Allah**, the most Beneficent and the most Gracious who enabled me to complete this research work. This would not be possible without the support, collaboration, and guidance from many people.

I would like to thank myself for not losing interest and keep going despite the hurdles throughout my research work. I am profoundly indebted to **Dr. Iftikhar Ahmad,** my project supervisor, for inspiring me to pursue this study.

I am grateful to other committee members **Dr. Umair Sikander** and **Dr. Muhammad Ahsan** for their valued guidance and suggestion. This completion of my work would not have been possible without them.

Furthermore, a very special note of thanks and appreciation goes to my **family** who prayed for me and encouraged me during all this period and the final stages of my research has provided me with moral support to complete my research work.

List of Abbreviations

Nomenclature

Computational fluid dynamic	CFD
Artificial Neural Network	ANN
Relative Exergy Array	REA
Heat Exchanger Network	HEN
Relative exergy Destroyed Array	REDA
Blast Furnace	BF
Height of the Blast furnace	H
Diameter of the Blast Furnace	D_f
Inlet Temperature of Oxides	T_{oin}
Inlet Temperature of Fluxes	T_{fin}
Tuyere Diameter	D_t
Lid Diameter	D_l
Blast rate oxygen	$\dot{m}_{O_2}$
Heat of Formation	ΔH_f
Physical exergy	E^{ph}
Chemical exergy	E^{ch}
Mixing exergy	E^{mix}
Molar Flow	$\dot{n}$
Effective diffusivity	D_{eff}
Reaction rate constant	k
Equilibrium constant of reaction	K_e
Ideal Gas Constant	R
Internal energy	e
Enthalpy	h
Enthalpy of Formation	$\bar{h}$
Standard temperature	To

Standard pressure	Po
Million Tones per Anum	Mtpa
Tons of Oil Equivalents	TOE
Gross Domestic Product	GDP
Two Dimensional	2-D
Three Dimensional	3-D

Subscripts

O_2	Oxygen
CO_2	Carbon dioxide
C	Carbon
Three Dimensional	3-D

Greek Letters

a_{melt}	Melting factor
β	Heat transfer from air to solids
φ	Juttner Modulus
γ	Bias factor
$\bar{G}$	Output of ANN
$\in$	Void fraction
ρ	Density

Table of Contents

Chapter 1 Introduction 1

1.1 Thesis Outline 4

1.2 Theoretical Background 4

1.2.1 Iron making Process in Blast furnace 4

1.2.2 Types of Furnaces 6

1.3 Reaction Kinetics of Iron Formation Process in Blast Furnace 7

1.3.1 The reduction of a single oxide particle 7

1.4 Exergy 9

1.5 Reference Environment 10

1.6 Exergy Balances 11

1.6.1 Components of Exergy 12

1.7 Artificial Neural Network (ANN) Modeling 13

1.7.1 ANN background 14

1.7.2 Training and testing of ANN 15

Chapter 2 Literature Review and Objectives 16

2.1 Modelling of a blast furnace 16

2.2 Exergy Quantification by Simulation 17

2.3 Comparison of Exergy Analysis Tools 18

2.4 ANN as a predictive tool 19

2.5 Objectives 20

Chapter 3 Methodology 21

3.1 Simulation Procedure in MATLAB 22

3.1.1 Assumptions 22

3.1.2 Governing Equations 23

3.1.2.1 Ergun's Pressure Drop equation 23

3.1.2.2 Steady State equation 24

3.1.2.3 Reaction rate constant 24

3.2.2.4 Effective heat transfer coefficient 25

3.2.3 Modeling in MATLAB 26

3.2.3.1 Discretization 26

3.2.3.2 Initialization of Parameters and Variables 27

3.2.3.3 Calculations in MATLAB 28

3.2.3.4 Exporting from MATLAB 31
3.2.4 Application of ANN 32
Chapter 4 Results and Discussion 34
4.1 MATLAB Modeling Results and Validation 34
4.1.1 Air direction Profiles 34
4.1.2 Oxygen Concentration 35
4.1.3 Velocity Magnitude 37
4.1.4 Stream Function 38
4.1.5 Temperature 39
4.1.6 Exergy 41
4.2 ANN Model result 43
Conclusions and Recommendations 45
References 46

List of Figures

Figure 1.1: Iron and Steel making techniques and Share Globally.....1
Figure 1.2: GDP and Energy breakdown of Pakistan 2016-17.....2
Figure 1.3: Energy consumption breakdown of a typical Foundry 3
Figure 1.4: Blast Furnace Diagram 4
Figure 1.5: Reaction zones within BF with Temperature.....5
Figure 1.6: Different types of furnaces 6
Figure 1.7: Process flow diagram of Blast furnace.....7
Figure 1.8: Reduction of Single oxide.....8
Figure 1.9: Interaction of energy, entropy, and exergy.....10
Figure 1.10: Inflow and outflow of energy, exergy, and entropy through a system....11
Figure 1.11: Single Neuron's Computation depiction.....14
Figure 1.12: Architecture of ANN.....15
Figure 3.1: Process flow description of MATLAB 22
Figure 3.2: Grid Discretization 27
Figure 3.3: Null Matrix 28
Figure 3.4: Nested For Loop Layout 30
Figure 3.5: Model Development Schematic 33
Figure 4.1: Air profiles in the furnace (a) results (b) literature 35
Figure 4.2: Contour plots of Oxygen Concentration (a) Simulation results (b) Literature Fluent (c) MATLAB literature.....36
Figure 4.3: Velocity Magnitude (a) Simulation results (b) Literature Fluent (c) MATLAB literature 38
Figure 4.4: Stream Function (a) Simulation results (b) Literature Fluent 39
Figure 4.5: Temperature (a) Simulation results (b) Literature Fluent 40
Figure 4.6: Temperature zones profiles by diameter along the height 41
Figure 4.7: Exergy contours (a) Total exergy (b) Physical exergy (c) Kinetic exergy (d) Potential exergy 43
Figure 4.8: ANN regression plots (a) Charge temperature (b) Gas temperature (c) Concentration of Oxygen (d) Velocity (e) Total Exergy 43

List of Tables

Table 3.1: Parameters of Furnace…… 21

Chapter 1

Introduction

Overall country's economic development depends upon the development of the Iron and Steel manufacturing sector of the country [1]. It reflects the infrastructure development capability of any country. It has been observed by various studies that about 5 percent of the total energy consumed around the globe is utilized by the Iron and steel sector [2-6]. A continuous steel making process includes three major processes named Iron making followed by steel making and post-processing like shaping, coating, and other treatments. The steel making process mainly depends upon the reduction of iron from its ore. This process is performed in different ways in which reduction through blast furnace is the most common and widely used method. Other process includes gas-based reduction, coal-based reduction, and electricity-based reduction. These methods are applicable in the areas where iron ores and coal have not much quality to be treated in the Blast Furnace. These methods are also considered where the inexpensive natural gas reserves are of much abundance and the quantity required is much lower. For intensive production, a large demand for iron, the only solution is a blast furnace.

While considering the global consumption of iron, about 94 percent of the iron is produced through Blast Furnace. Figure 1 shows the study performed by World Steel Organization in 2012 summarizes that about seventy percent (70 %) of the total steel produced globally is done through the blast furnace- oxygen method of steel making [7].

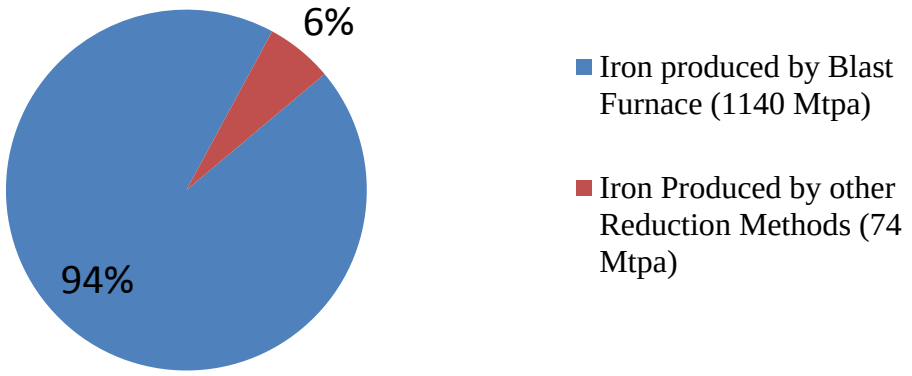

Figure 1.1: Iron Making Techniques and Share Globally (Steel Statistical Yearbook and World Steel Organization 2012) [8]

Pakistan being a developing country also requires enhanced Iron and Steel production. The recent statistics regard the country to be more dominant in the industrial sector as well. During the fiscal year 2016 - 17, the industrial sector has contributed 18% of the GDP which is 2% more than that of the agricultural sector.

This also increases the country's overall energy demand as well. From 1996 to 2007, the energy consumption of Pakistan has been increased by 1.44 quadrillion BTU having an average annual rate of increase of 3.38 % [9]. By the statistical data collected annually, it is always evident that the energy requirement by the industrial sector has always been greater than that of agriculture. In 2015, the total energy supply was 93.91 million tons of oil equivalents (TOE), within which 23.77 percent of energy was consumed by industries and 0.98 percent was utilized by agriculture. Within the industrial sector, Iron and steel manufacturing units are contributing 64.4% of the sector's contribution towards GDP or 13.45% of total GDP thus; improving energy consumption in this sector would effectively decrease the energy deficit of the country.

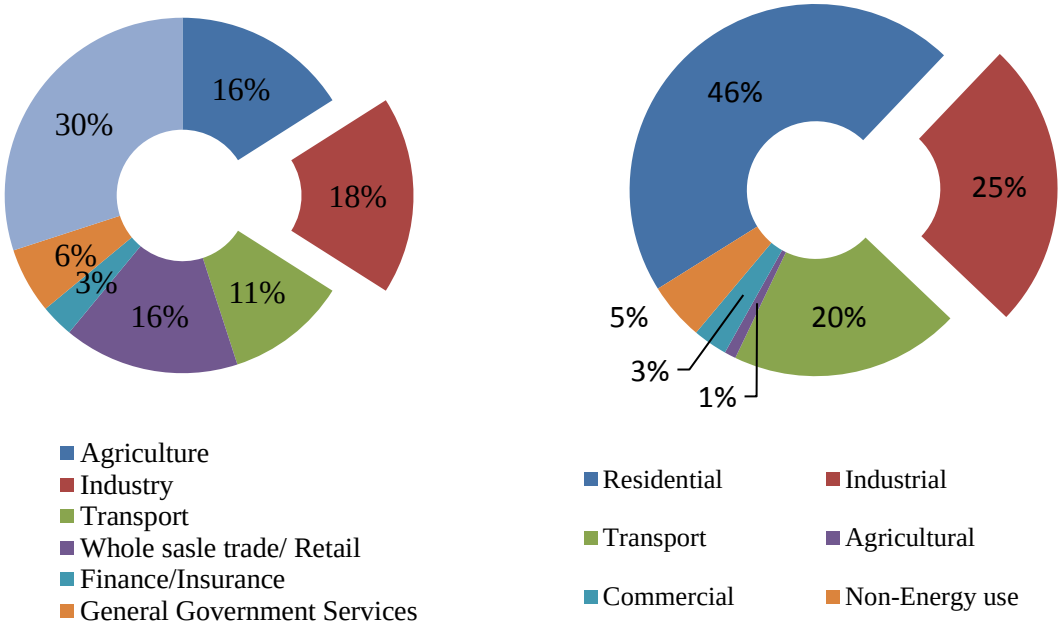

(a) (b)

Figure 1.2: (a) GDP breakdown of Pakistan 2016-17, (b) Energy breakdown of Pakistan 2016-17 [10]

The energy consumption by different processes within the Iron and Steel manufacturing setup is summarized in figure 1.3. It is much evident from the graph

that most of the energy is utilized during the melting of the metals. This reflects the importance of the improvement of energy efficiency and optimization of the Blast furnace which is directly involved in the melting of iron in the Iron and Steel industry.

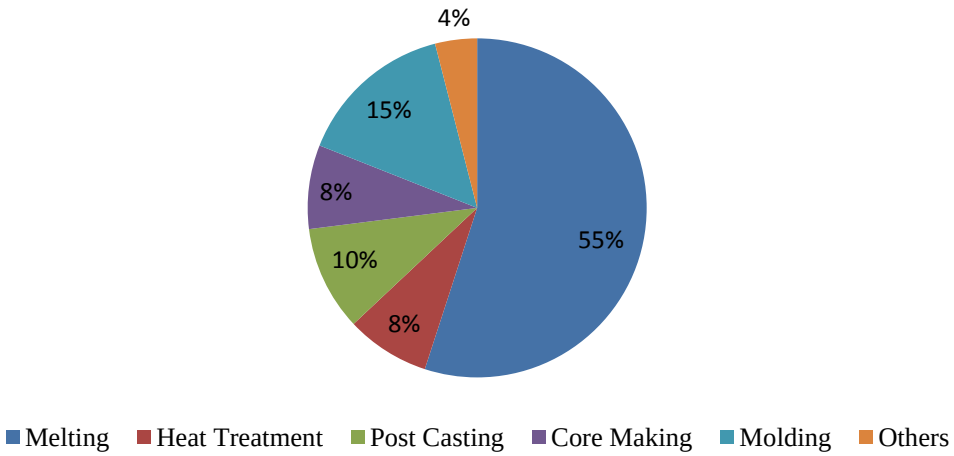

Figure 1.3: Energy consumption breakdown of a typical Foundry

With the development of the concept of energy analysis, it is much helpful to develop an artificial but similar environment as that of original process geometry. This concept helps to solve such problems in less time as well as avoid frequent operational iterations of the process. Using artificial intelligence tools on the modelled data helps to study the operation for different conditions and parameters hence helps in predictive analysis of the process easy.

In this work, exergy analysis of the main component of Iron manufacturing i.e. Blast furnace for melting is modelled in MATLAB. Using the data from the literature, the model of the furnace was developed. The dimensions and operating parameters were taken from the literature. The cross-section of the blast furnace is shown in figure 1.4. During the reduction of iron from iron oxide, the charge undergoes a series of reactions. The iron ores along with coke and fluxes as fuel are introduced from the furnace top while the blast of hot air is introduced in the furnace through the set of tuyers along the circumference of the furnace at the bottom. The iron ore introduced from the top undergoes a series of reactions to give iron at the bottom with slag floating over it which is collected separately.

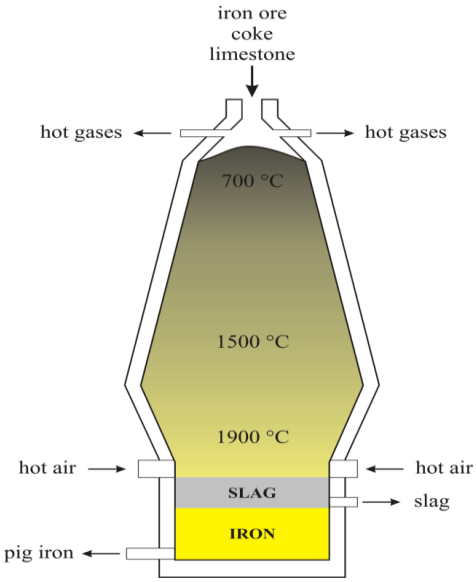

Figure 1.4: Blast Furnace Diagram [11]

1.1 Thesis Outline

Basic theoretical concepts, reaction kinetics, exergy, and ANN architecture are discussed in Chapter 1. Literature survey explaining the use of MATLAB and ANN in various previous works and objectives are explained in Chapter 2. The methodology of simulation in MATLAB and steps of Modeling in MATLAB with the procedure of ANN are discussed in detail in Chapter 3. Results are presented and validated in Chapter 4. While in the end the conclusive comments and future recommendations regarding this project are given after chapter 4.

1.2 Theoretical Background

1.2.1 Iron making Process in Blast furnace

The process of Iron production includes three continuous reduction reactions of Iron oxides within the BF. As preheated air enters the furnace from the bottom, it reacts with the coal introduced from the top of the furnace, producing carbon mono-oxide (CO). These sets of reactions have a specific heat of formations represented below along with the reactions [12].

$$C_{(s)} + O_{(g)} = CO_{(g)} \quad (1.1)$$

$$\Delta H_f = -99 KJ/Mol$$

This carbon mono-oxide reacts with the feed oxide and reduces it into ferrous Oxide (FeO). In the final reduction of Iron, this ferrous oxide is further reduced into Iron producing Carbon dioxide (CO_2) as by-product.

$$3Fe_2O_{3(s)} + CO_{(g)} = 2Fe_3O_{4(l)} + CO_{2(g)} \quad (1.2)$$

$$\Delta H_f = -52.869\ KJ/g - Mol$$

$$Fe_3O_{4(l)} + CO_{(g)} = 3FeO_{(l)} + CO_{2(g)} \quad (1.3)$$

$$\Delta H_f = -36.25\ KJ/g - Mol$$

$$FeO_{(l)} + CO_{(g)} = Fe_{(s)} + CO_{2(g)} \quad (1.4)$$

$$\Delta H_f = -17.305\ KJ/g - Mol$$

During this process, the limestone is also added as flux along with iron oxide from the top to remove the impurities. Calcium Carbonate $(CaCO_3)$ undergoes dissipation reaction and splits into Calcium Oxide (CaO) and Carbon dioxide (CO_2). This calcium oxide (CaO) reacts with the impurities present in the charge materials like Silica (SiO_2) to form Calcium Silicate $(CaSiO_3)$ commonly known as slag which is collected from the bottom of the furnace. The molten metal being highly dense remains down while slag, less dense, floats and is being collected separately.

$$CaCO_{3(s)} = CaO_{(l)} + CO_{2(g)} \quad (1.5)$$

$$CaO_{(l)} + SiO_{2(s)} = CaSiO_{3\ (s)} \quad (1.6)$$

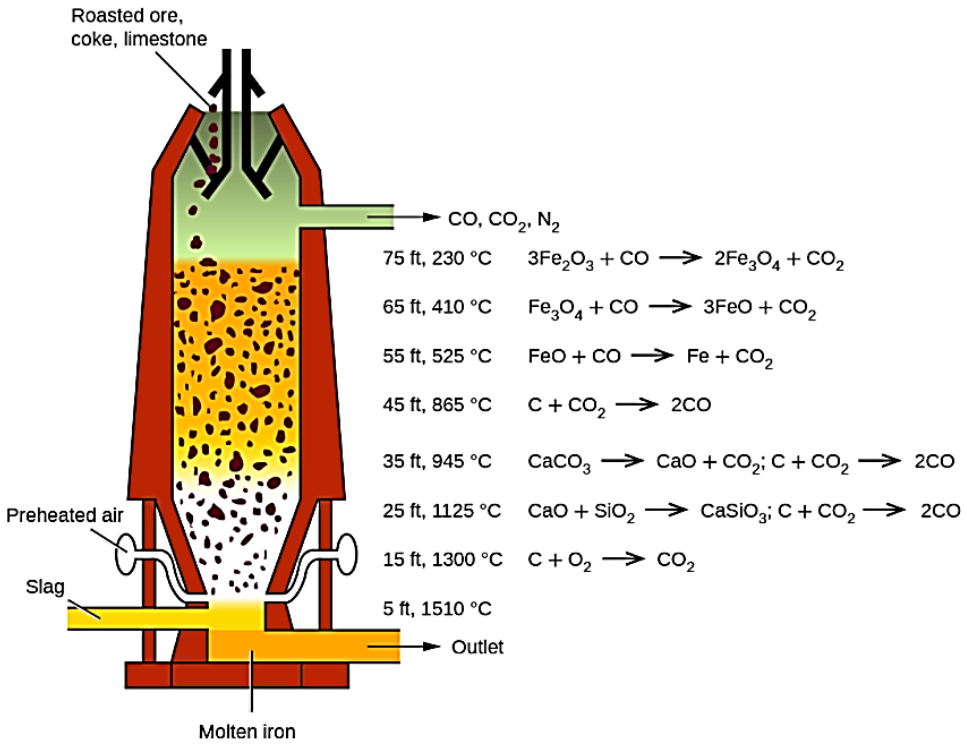

Figure 1.5: Reaction zones within BF with Temperature [13]

Designing a blast furnace is yet not an easy task to perform. It requires a lot of parameters to be accounted for while modelling blast furnaces in any modelling software. Modelling a full-scale furnace is tedious as it requires much time and high-performing operating systems. So, it is easy and feasible to model a small-scale furnace with the same reaction kinetics. These small-scale furnaces are often regarded as cupollette. The main objective of this research is to obtain the same processes inside the furnace to develop a predictive tool afterward.

1.2.2 Types of Furnaces

The furnaces producing Iron can be divided into three types based on their production capabilities which affect the required height of the furnace according to the requirement. For having production of about tones per hour, the furnace of height about 20-30 meters is used. These furnaces are regarded as blast furnaces. These furnaces need to be run continuously unless their interior lining wears off which calls for a shutdown.

The second and third iron making furnaces are not required to be run continuously and can be shut down when the required amount of iron is produced. Their geometries are different in the way that they have straight rectangular geometry and do not have and bulge as in the blast furnace. The height is the major difference while other geometrical aspects are scaled down according to the size but are beyond the scope of this work. This helps to have the same geometry according to the requirement as shown in figure 2.2. Figure 2.3 highlights the different types of furnaces.

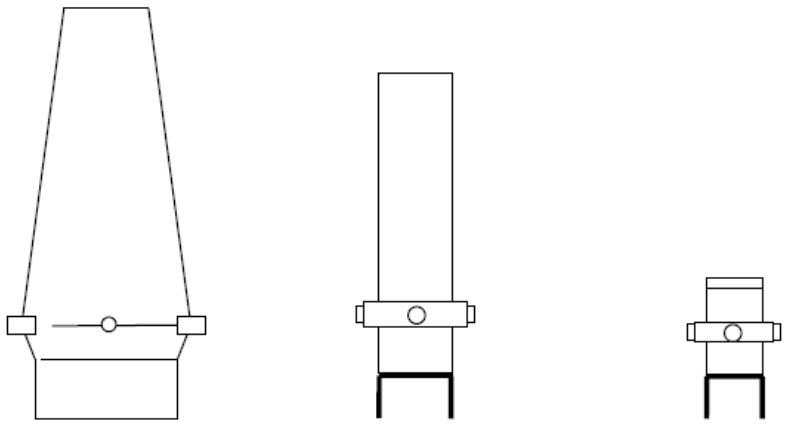

Figure 1.6: Different types of furnaces Blast furnace (left), Cupola (Middle), Cupollette (right) [14]

1.3 Reaction Kinetics of Iron Formation Process in Blast Furnace

Usually, a spherical pellet is used in mathematical modeling due to its simple geometry. So, a similar pellet can be used while studying Iron oxide reduction by CO [12]. In this section, the shrinking core mode1which was developed in the study of pellet reduction is briefly reviewed. Rate controlling steps and values of rate constants reported in the literature are discussed.

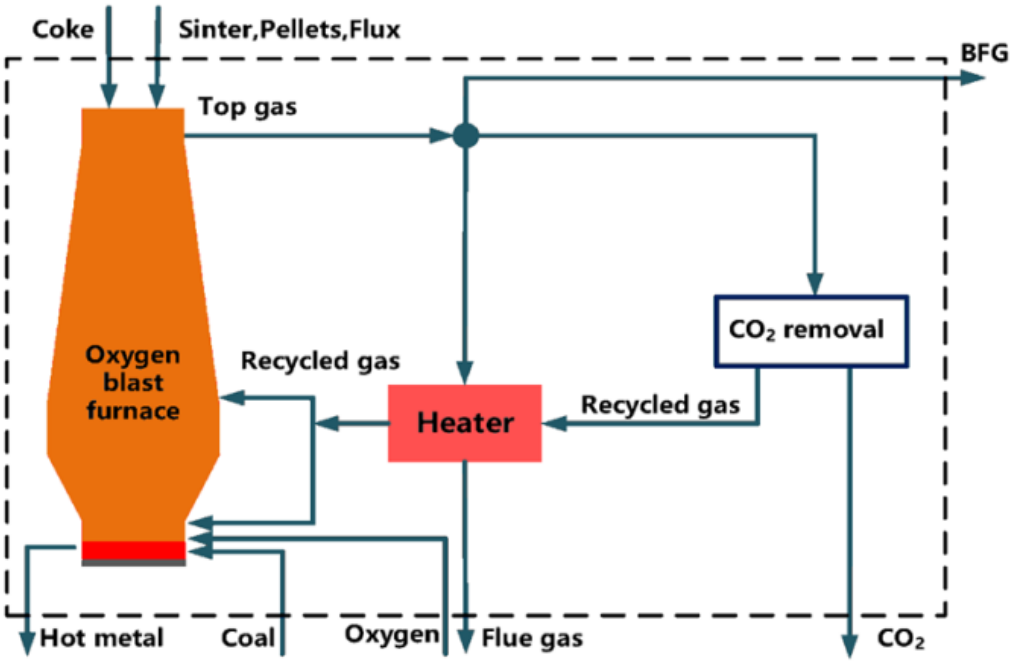

Figure 1.7: Process flow diagram of Blast furnace [15]

1.3.1 The reduction of a single oxide particle

The reduction of the oxides can be studied by considering a suspended spherical sample of the oxide in the gas with known temperature and composition flowing with typical velocity. In this way, the weight loss can be monitored. The weight loss data for the oxide is analyzed by performing experimentation for three different conditions which include isothermal, solid/solid interface reaction where solid/gas reaction is occurring, and specimens with high density [16, 17]. Figure 1.5 represents the single oxide reduction of Iron.

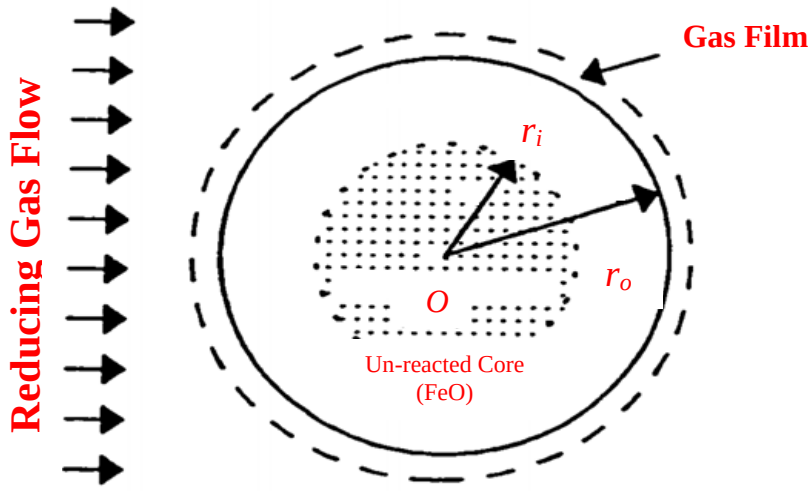

Figure 1.8: Reduction of Single Oxide [12]

It can be observed in the figure that the system of iron oxide reduction consists of three phases which include the unreacted solid reactant in the core, the porous layer of iron as solid, and the gaseous phase as the outermost layers. During reduction, oxygen is removed from the wustite at its interface with iron which results in weight loss. This process involves the following steps:

a. Reactant transport from bulk to the external surface of the particle i.e. CO to the Iron core.
b. Diffusion of the reactant from middle porous surface to the core i.e. CO transport to the Iron/wuistite interface.
c. Reduction of the core by reactant to the pure core and by-product (i.e., wuistite) converts into Iron producing carbon monoxide (CO) as a by-product.
d. Diffusion of by-product out from porous layer i.e. CO diffusion.
e. Transport of by-product to the bulk gas (i.e., CO) transport

These steps can be mathematically represented as [18],

i. Transfer of mass through gaseous film in steps "a." and "e." (i.e., the molar flux of reactant (CO) from bulk to gas phase) is given by:

$$\dot{n}^{m}_{CO} = -h_{CO} \cdot 4\,\pi\, r_O^2 (C^{b}_{CO} - C^{O}_{CO}) \tag{1.7}$$

Similarly, the molar flux the other way around can be given by,

$$\dot{n}^{m}_{CO_2} = -h_{CO_2} \cdot 4\,\pi\, r_O^2 (C^{b}_{CO_2} - C^{O}_{CO_2}) \tag{1.8}$$

where,

$\dot{n}^{m}_{CO}$ = molar flow of CO from bulk to the exterior in mole/s,

$\dot{n}^{m}_{CO_2}$= molar flow of CO from exterior to bulk gas in mole/s,

$\boldsymbol{h_{CO}}$ = mass transfer coefficient of Carbon monoxide in m/s,

$\boldsymbol{h_{CO_2}}$ = mass transfer coefficients for Carbon dioxide in m/s,

$\boldsymbol{C^{b}_{CO}}$ = Carbon monoxide concentration at the bulk phase in mole/ $m^{3,}$

$\boldsymbol{C^{O}_{CO}}$= Carbon monoxide concentration at exterior in mole/ $m^{3,}$

$\boldsymbol{C^{b}_{CO_2}}$= Carbon dioxide concentration at the bulk phase in mole/ $m^{3,}$

$\boldsymbol{C^{O}_{CO_2}}$= Carbon dioxide concentration at exterior in mole/ $m^{3.}$

ii. In steps "b." and "d.", the molar flows of carbon monoxide (CO) and carbon dioxide (CO_2) given by $\dot{n}^{m}_{CO}$ and $\dot{n}^{m}_{CO_2}$respectively are calculated by diffusion from the porous layer as,

$$\dot{n}^{D}_{CO} = -D_{effCO}\, 4\pi\, r_i^2\, \frac{\partial\, C_{CO}}{\partial\, r} \quad (1.9)$$

$$\dot{n}^{D}_{CO_2} = -D_{effCO2}\, 4\pi\, r_i^2\, \frac{\partial\, C_{CO_2}}{\partial\, r} \quad (1.10)$$

where,

$\mathbf{D_{effCO}}$ = Effective diffusivity of carbon monoxide in m^2/s

$\mathbf{D_{effCO2}}$ = Effective diffusivity of carbon dioxide in m^2/s

iii. In step "c.", the removal of oxygen from FeO interface with Fe is considered to be a first-order reversible reaction with reaction represented as,

$$\dot{r}_o = -k\, 4\, \pi\, r_i^2 (C_{CO} - C^{O}_{CO_2}/K_e)) \quad (1.11)$$

where,

$\dot{r}_{\mathbf{o}}$ = Oxygen removal rate in mole/s,

$\mathbf{k}$ = reaction rate constant in m/s,

$\boldsymbol{K_e}$ = equilibrium constant of the reaction.

1.4 Exergy

The term **exergy** was coined in 1956 by Zoran who combined the meaning of two Greek words '**ex**' and '**ergon**' which when combined means "**from work**". Exergy can be well illustrated and defined by the statement,

The amount of possible work is obtainable by bringing a matter from its initial state through a reversible process to a condition of thermodynamic and chemical equilibrium with the reference environment referred to as a dead state [19].

Exergy quantifies the actual amount of work so it can be set as a defining standard. The energy losses due to the irreversibility of a real system appear in the entropy form. While Entropy is the unavailable amount of thermal energy present in the system to do work so, the relation between exergy and entropy production is shown by the thermodynamics second law [20]. Hence, the generation of entropy links directly to the loss of exergy leading towards degradation or loss of exergy in any real-time process. However, it is much desirable in any process to have maximum exergy output from the input provided to the system.

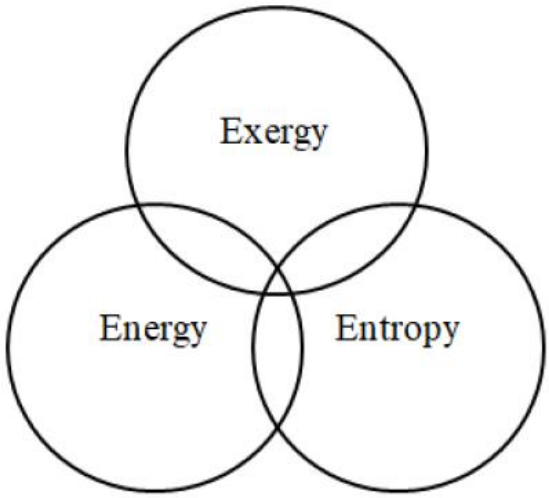

Figure 1.9: Interaction of energy, entropy, and exergy

1.5 Reference Environment

In this reference environment, there must be no difference in the values of temperature, pressure, kinetic, potential, and chemical potential energy among each of the components of the reference environment. In literature, a lot of reference environments have been discussed while the reference environment in this work states following standard values,

$$\text{Standard temperature} = T_o = 298.15 \text{ K}$$

$$\text{Standard pressure} = P_o = 101.325 \text{ kPa}$$

The standard values used are stated by Szargut et. al [21].

Any thermodynamic body or component when brought to equilibrium with the environment, it requires full thermodynamic equilibrium with it which includes thermal, chemical, and mechanical as well.

1.6 Exergy Balances

The Exergy study is governed by the first and second law of thermodynamics. The first law of thermodynamics describes that energy can never vanish; while the second law of thermodynamics states that heat energy cannot be fully brought into service when it is involved with the real system. The wasted energy appears in the form of entropy due to the irreversibilities of the processing system. The relation of energy, exergy, and entropy is shown in Figure 2.5.

The energy flowing in and out are equal in amount, as stated by the first law of thermodynamics; on the other hand, the quantity of entropy moving out is larger than the moving in according to the law of entropy increase. The quantity of exergy moving out is lesser than the moving in. This is due to a portion of exergy is lost within the system due to irreversibilities that appear in the form of entropy.

A mathematical model of exergy is given by the following equation [18].

$$E_{ex(Tot)} = K.E + P.E + (h - h_0) - T(S - S_o) + E_{ex(chem)} \quad (1.12)$$

$$E + H = \text{Work } (1^{st} \text{ law of thermodynamics})$$

$$S = S_{gen} \ (2^{nd} \text{ law of thermodynamics})$$

The first three terms of the total exergy equation (i.e. 1.12) are the portion represented by the first law of thermodynamics while the fourth term is the portion represented by the second law of thermodynamics. It can be observed that the exergy equation includes the first as well as the second law of thermodynamics to find the maximum amount of work attainable from a system.

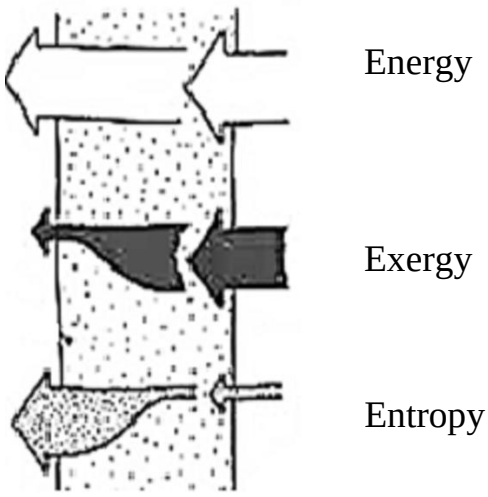

Figure 1.10: Inflow and outflow of energy, exergy, and entropy through a system

1.6.1 Components of Exergy

If the stream under consideration is free from nuclear, electricity, magnetism, and surface tension, the exergy of the stream can be divided as,

$$E=E^{K} + E^{P} + E^{ph} + E^{O} \quad (1.13)$$

where,

E = total molar exergy,

E^{K} = molar kinetic exergy,

E^{p} = molar potential exergy,

E^{Ph} = molar Physical exergy,

E^{O} = molar Chemical exergy [22].

The amount of useful work attainable while bringing the component of the system to the dead state from the initial state via reversible process regarding the reference environment is the total exergy [23].

The thermo-mechanical part of the total exergy represents the Physical exergy. It is the amount of work to bring the component or material to a dead state at reference environment (T_O, P_O) from the original or initial state (T, P) under thermodynamic conditions via a reversible path [24].

Mathematically, molar physical exergy can be written as, [19]

$$E^{Ph} = RT_o \sum_{i=1}^{n} Cp_i^{mean} \ (T_i - T_o - T_o \ln\left(\frac{r_i}{r_o}\right)) \quad (1.14)$$

$$Cp_i^{mean} = \int_{T_1}^{T_2} Cp_i \, dT \quad (1.15)$$

$$Cp_i \left(\frac{j}{mol.K}\right) = a_i + b_i T + c_i T^2 + d_i T^3 \quad (1.16)$$

where,

a_i, b_i, c_i, d_i = heat capacity coefficients at each point of furnace,

R = ideal gas constant at each point of furnace,

P_i= Partial Pressure of each component at each point of the furnace,

T_i = Temperature of each component at each point of furnace [25].

The maximum attainable work from any matter, while bringing it from initial thermos-mechanical as well as chemical equilibrium to the dear reference state is defined as chemical exergy [25].

Mathematical representation of chemical exergy of a component stream is given as;

$$E^{ch} = \sum_{i=1}^{n} V_i \bar{G}_i(Reactants) - \sum_{i=1}^{n} V_i \bar{G}_i(Products) \quad (1.17)$$

$$\bar{G}_i = G_f^o + \left\{ \bar{G}_{i(T,P)} - \bar{G}_{i(T_o,P_0)} \right\} \quad (1.18)$$

The kinetic and potential exergies fully represent the ordered forms and hence are all fully convertible into work. Kinetic and Potential exergies can be represented with respect to the reference environment in the equation below as [22];

$$E^K = m_o \frac{{c_O}^2}{2}$$

(1.19)

$$E^P = m_o g_E Z_o \quad (1.20)$$

where;

m_O = mass flow rate of the bulk stream,

C_O= Bulk velocity,

Z_O= Altitude above sea level.

1.7 Artificial Neural Network (ANN) Modelling

1.7.1 ANN background

ANN is a set of neurons working together to predict the output of a typical process computationally. It receives data in the form of input which is stored in the form of scaled inputs in a neuron, makes its independent calculations, and finally predicts the output of the process [26]. Weight is assigned to each neuron regarded as an autonomous identity, a bias term, and a transfer function. For instance, the computation of a single neuron is shown in figure 1.11 below,

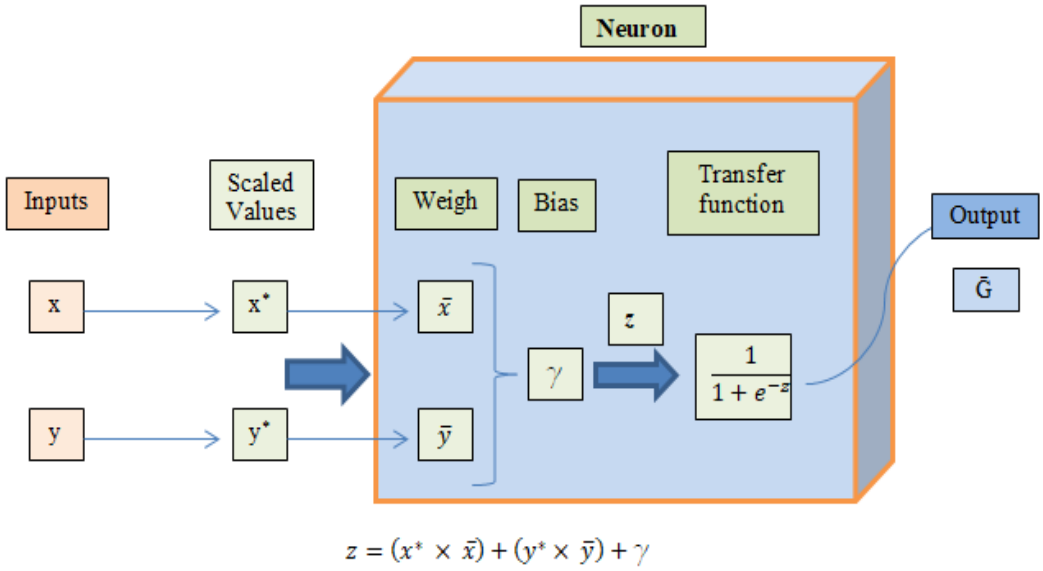

Figure 1.11: Single Neuron's Computation depiction

It can be observed from the figure that the output of ANN is calculated by adding up the products of every input's scaled values and weight to which bias value is added. This value is then applied to the transfer function which is selected according to the process. For instance, the '*log sigmoid function*' is used as a transfer function in figure 1.11. The final output computed from the ANN can be given by the equation 1.21.

$$Output = S[c_j + \sum_{j=1}^{i=n}(a_{ij}x_i)] \quad (1.21)$$

where;

a_{ij} = weight of each scaled input variable,

c_j= Bias factor of jth neuron,

x_i= Scaled input.

1.7.2 Training and Testing architecture of ANN

Usually, by the architecture, the ANN is divided into three layers named input, hidden, and output layers. Hence, figure 1.11 can be summarized in figure 1.12 as,

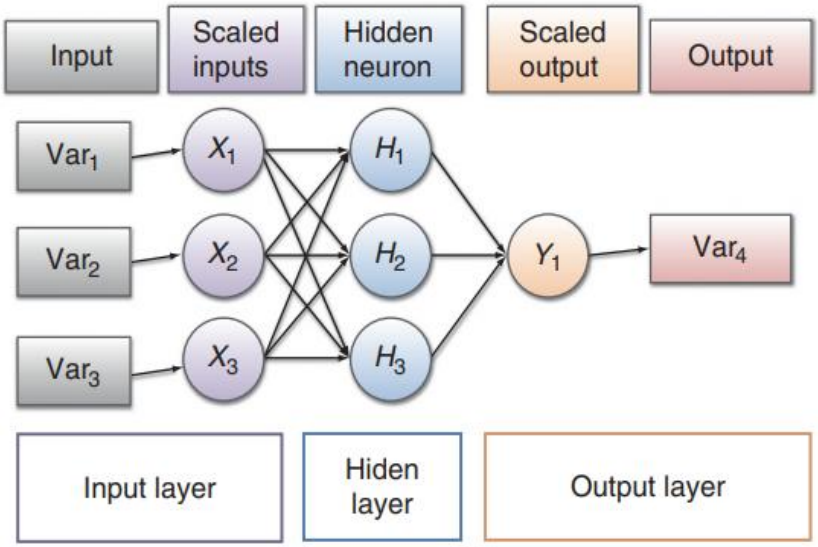

Figure 1.12: Architecture of ANN [27]

Once the architecture is well understood, the model for ANN is trained for the known inputs and output values. During the training of the ANN, the model continuously assigns values to the neuron until it reaches the desired allowable error in bias factor and hence, a good relationship is established between input and output data. The data obtained from the process is usually divided into two subsets randomly. One of the subsets is used for training the model while the other set helps in validating the model. Basherr et al. [28] discuss the architecture of the ANN in detail.

Chapter 2

Literature Review and Objectives

This chapter presents the literature review of the blast furnace modeling, exergy quantification, use of the artificial neural network for prediction of its parameters and the objectives of this research.

2.1 Modelling of a blast furnace

The literature indicates work by Dong et al [29], Dmitriev [30], and Jin et al [31] in the field of mathematical modelling of the Blast furnace. Dong et al concluded that burden distribution is related with the furnace efficiency and its stable operation as well [29]. Dmitriev explained the two dimensional modeling of BF in a book. He categorized the mathematical models and use of complex mathematical models for commercial uses as well [30]. Junpeng [31] used fuzzy logic to improve the quality of molten steel produced by the furnace. Sun et al [32] also worked for hybrid model for data driven blast furnace gas prediction. Mahanta et al modelled blast furnace noisy data set for its energy optimization [33]. Similarly, Saxén et al predicted silicon content in the hot metal using data based model of the blast furnace [33]. The study by Zhou et al. also helped in prediction of molten iron quality indices in the BF [34]. Zhou et al [35] also used nonlinear subspace modeling for prediction and control of the molten metal through the blast furnace. Modeling of the furnace and prediction through the model is a unique futuristic approach for numerous process equipments. The hybrid approach of prediction of the process based upon FP model is significant to have process insight and change process accordingly. While the grey box or data driven models are unaware of the process insight and hence the process operational and geometrical parameters cannot be changed if required while optimizing.

Using MATLAB as a computational fluid dynamics tool is much handy as compared to other simulation soft wares as most of the process parameters and variables remain in hand and are easy to change for the user. It also helps to use numerous optimizations as well as predictive tools built in the MATLAB for the process as well and hence the difficulty of interfacing different soft wares is overcome. Various researches can be

found in the literature following this trend. For example, Acosta-Herazo et al. [36] performed MATLAB-based simulation and modeling of the photocatalytic reactor. They found the graphical user interface of MATLAB to be more user-friendly and efficient to solve such complex problems for environmental problems. Ismail et al. [37] used MATLAB as a simulating tool to model the production of hydrogen through the photovoltaic cell and validated their results as well. Prades et al. [38] used MATLAB to model the transport phenomenon in a biofilm reactor in two dimensions. They validated the results obtained from their study with the results of the same scenario in ANSYS Fluent and found the results to be much comparable. Logist et al.[39] provides detailed guidelines for modeling chemical processes involving non-linear convection reaction-diffusion partial differential equations (PDE's). They also modelled complex reverse flow reactor in the environment of MATLAB and successfully combined the model with the optimization tool as well. Spiegel et al. [40] published a book illustrating in detail the fuel cell modeling in the MATLAB environment. They found its interface much user friendly and used optimization tools in MATLAB as well. They incorporated every aspect of the fuel cell and hence made the engineers, researchers, and manufacturers have the best-desired product easy to attain. Molina et al. [41] performed the parametric study and hence optimized the chemical kinetics of the batch reactors. Hence, MATLAB is found to be very handy and user-friendly to perform fluid dynamic simulations on chemical processes.

2.2 Exergy Quantification by Simulation

Exergy efficiency based studies has been getting attention of researcher because it is very useful in identification of the location, cause as well as the magnitude of the inefficiencies in the system [42]. Exergy quantification is the most advanced technology to optimize the plant or process thermo-economically. Unlike energy analysis, exergy incorporates second law of thermodynamics and hence is the only tool to compare the process. Zhang et al performed exergy analysis on the top gas recycling oxygen blast furnace [43]. They based their study on two different composition of charge and were successful to increase efficiency by 1-4 percent. Guo et al [44] performed exergy based analysis on the blast furnace operated by natural gas. They deduced that operating blast furnace by natural gas helps to increase its productivity, reduce silicon content in molten metal and carbon emission but reduce its exergetic efficiency. The exergy efficiency of the blast furnace was seventy percent with best

results by using pulverized coal and pre heating of the charge material which also helps in saving in coke [45]. While comparing the rotary hearth furnace (RHF) and Waelz Kiln process, the RHF requires less resources however, it has more exergy inputs. The optimized Waelz kiln was found to be 10 percent while the RHF was 21-23 percent exergy efficient [46]. Similar study of the silicon furnace shows that volatiles and electrodes accounts for about 8-10 percent of exergy destruction. While the overall exergy was reported 30 percent [47]. Hasan et al [48] analyzed the annealing furnace for metals for exergy and economics. They found that the combustion chamber of the annealing furnace is about 12.9 percent exergy efficient while the overall exergy efficiency of the furnace was found to be 7.3 percent. The most exergy destructive units were found to be annealing chamber followed by the combustor. The overall exergy efficiency for the electric arc furnace was reported to be about 55 percent [49]. Calise et al. [50] performed exergy analysis using MATLAB on a hybrid solid oxide fuel cell (SOFC)- Gas turbine. They found the most optimized conditions to operate the turbine by using the predictive tool of MATLAB. Yousef Nezhad et al. [51] performed an exergy analysis of a solar water heater. They deduced that collector surface area is the most important factor in the performance of the solar heater. Dogbe et al. [52] performed exergy analysis based upon Aspen Plus simulation of the sugar mill. They found that the efficiency of the sugar mill can be very much improved by adopting single-stage crystallization with an integrated biorefinery. Ahmadi et al. [53] calculate the hydrogen production efficiency of the process along with exergy damages and efficiencies based on ocean thermal energy conversion systems. Ghorbani et al. [54] performed an economic analysis based upon energy and exergy on the integrated power generation system. They performed an analysis based upon MATLAB, HYSY, and TRANSYS soft wares according to their ease. Thus, exergy analysis helps in a lot of processes to have economical saving and optimization.

2.3 Comparison of Exergy Analysis Tools

Most of the process design and simulation is based upon mainstream soft wares like MATLAB, Aspen HYSYS/PLUS, and CHEMCAD. These applications lack the newly introduced concepts like exergy in built-in form. This space can only be covered by building user's codes or customized functions in flexible soft wares like Microsoft Excel, ANSYS Fluent, FORTAN, etc. These applications can also be linked by

interfacing tools with other data soft wares to analyze and optimize the process. Various examples of interfacing and developing various can be found in the literature. For example, Montelongo-Luna et al. (2011) performed exergy efficiency studies of distillation columns by using a relative exergy array (REA) [55]. Another research with a similar technique was performed by Munir et al. (2013) who evaluate the mono-chloro-benzene (MCB) plant and heat exchanger network (HEN) economically using relative exergy- destroyed array (REDA) [56]. Querol et al. (2011) use integrated Aspen PLUS and Microsoft Excel tools for exergy calculation and exergo-economic study and analysis of chemical processes [57]. Bahmanpour et al. (2014) used Aspen HYSYS and Aspen PLUS while studying exergy while converting methane gas to formaldehyde via methanol [58]. Huang et al. (2017) performed an exergy analysis of dissociation of crystalline nickel ferrite in a solar reactor. He concluded that with a decrease in temperature the physical exergy also decreases and a high rate of conversion increases the chemical exergy [59]. It has been found that most of the literature indicates CFD to be the latest tool for exergy analysis [60, 61]. It provides the user to have a process and equipment inside view while Aspen PLUS/HYSY, CHEMCAD, FORTAN, etc are limited to the process inlets and outlets exergy values. Another major advantage to use MATLAB for CFD modeling as well as to perform exergy analysis is that the user does not require exporting data to other software or interfacing them as the exergy formulae can be included along with other formulae and can be calculated easily with each iteration as well.

2.4 ANN as a predictive tool

ANN has been used as a predictive tool in many chemical processes. Some of the examples are summarized in this section. Bag et al. [62] predicted different parameters of blast furnaces using ANN by the industrial data. Golestani et al. [63] combined ANN with the model of electric arc furnace. Bilim et al. [64] predicted the compressive strength of the slag produced in the blast furnace for further use in various processes using ANN. David et al. used ANN to predict the silicon content in the slag using ANN for the blast furnace slag which helps to optimize the input conditions and hence making by-product useful as well. Most of the literature on using ANN in blast furnaces corresponds with an industrial database. But due to the lack of industrial data in this research, the validated model of the blast furnace was developed in MATLAB, and ANN was applied.

In this study, the first principle model of the BF is developed which provides a realistic insight of the furnace with respect to numerous process and operational variables of the furnace i.e. temperature, pressure of the charge, oxygen profile and velocity and exergy and energy profiles. Due to material and heat counter flow in the shaft section, the blast furnace process is regarded as high exergy effective [65]. Energy and exergy based evaluation of the system are two different types of analysis. The quantitative analysis of the system during energy transfer and conversion process based upon the first law of thermodynamics is regarded as energy analysis. Hence to fill the gap of quality of the energy, the second law of thermodynamics is used which incorporates utilization and loss of energy along with transfer and conversion. Hence, it is very helpful to evaluate the blast furnace much scientifically [66, 67]. Under standard states defined by the engineers, the exergy of the blast furnace is the maximum attainable work that can be drawn from it while the furnace maintains its equilibrium with the surroundings [68]. Later on, to speed up the calculations, the predictive tool i.e. ANN is used. This helps to reduce the computational cost and time of the first principle model developed prior to this.

2.5 Objectives

This work on furnace fulfills the following three objectives:

- Modeling and simulation of the furnace through MATLAB. This involves mathematical equations leading to the computational model.
- Validation of the results with literature with the same geometry and parameters to support future work.
- Exergy analysis of the furnace in the same computing environment i.e. MATLAB.
- Development of an artificial intelligence-based model for predictive analysis of the furnace using MATLAB.

Chapter 3

Methodology

The model followed during this research is of Casto et al [69] and Dartt Kevin [70]. Although the geometry of the furnace plays an important role, however, the geometry is considered to be rectangular like a large copula with dimensions mentioned in table 3.1. These dimensions according to Dartt Kevin correspond with the cupola furnace at Binghamton University.

Table 3.1: Parameters of Furnace

Parameter	**Symbol**	**Value**
Height of the Blast furnace	H	0.605 m
Diameter of the Blast Furnace	D_f	0.36 m
Inlet Temperature of Oxides	To_{in}	298 kelvin
Inlet Temperature of Fluxes	Tf_{in}	298 kelvin
Inlet Temperature of Air	Ta_{in}	298 kelvin
Tuyere Diameter	D_t	0.05 m
Lid Diameter	D_l	0.11 m
Blast Rate of Oxygen	$\dot{m}_{O2}$	0.224 kg/sec

MATLAB solves mathematical equations defined by the user to numerically solve the problems within the boundary conditions confined by the user. Results obtained from simulation help the engineers, designers, and researchers to develop, improve and optimize the designs accordingly. The main process of modeling through MATLAB is shown in figure 3.1.

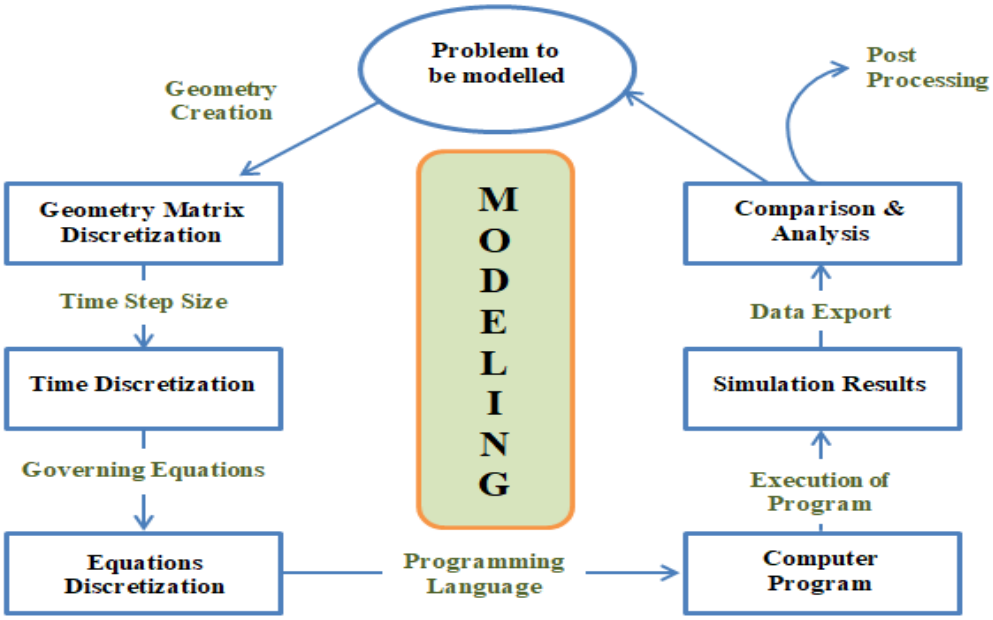

Figure 3.1: Process flow description of Modeling

3.1 Simulation procedure in MATLAB

While modeling in MATLAB, the following steps were followed,

3.1.1 Assumptions

During modelling of the furnace in MATLAB, some assumptions were made to make the model simple and easy to converge. These assumptions are summarized below.

- The first assumption is fulfilled while considering a scaled-down geometry of the furnace as a cupola. This helps to reduce the convergence time to be reduced a lot.
- It is also assumed that the furnace is a packed bed counter current reactor as the flow of the charge and air is on opposite sides [71]. This assumption helps to consider heat and mass transfer as well as the reaction kinetics. This packed bed reactor considers metal ore and charges material as packing material through which air passes.
- The second assumption helps to lead the problem toward Ergun's Pressure drop equation which considers the viscosity change as well as the change in inertia as fluid moves through the packed bed reactor. This helps to reduce the computational time a lot during iterative calculations. Ergun's equation is described in detail in the next section.

- It is also assumed that oxygen is the limiting reactant and charge (coke) is provided continuously. As oxygen is the energy-providing species in the reaction, it plays a key role in the combustion process. This assumption helps to calculate the reaction rates and indirectly the number of moles of oxygen consumed. Hence, the heat provided to the system can be evaluated by the number of moles of oxygen. The particles of the charge coke are considered to be having uniform temperatures with the air surrounding it in the furnace [72].
- It is assumed that heat transfer between the gasses and the solids is majorly due to convection as it plays a vital role while calculating the heat transfer coefficients.
- It is assumed that a very small amount of carbon monoxide is available in the furnace i.e. most of the carbon undergoes full combustion in the furnace.
- The charging materials are vertically injected hence are considered to be moving vertically always.
- The void fraction and size of the particle remain constant throughout the reactions.
- The only heat loss is due to the gas leaving the furnace.

3.1.2 Governing Equations

The equations used in MATLAB, while modelling, are summarized below. These equations were discretized for each cell of the matrix and hence calculated.

3.1.2.1 Ergun's Pressure Drop Equation:

The pressure drop within the furnace can be evaluated by the equation given below [73],

$$\frac{\nabla P}{D_f} = \frac{150(1-\epsilon)^2}{\epsilon^3\, d_c^2}\,\bar{V} + \frac{1.75\rho_g(1-\epsilon)^2}{\epsilon^3\, d_c}\,|\bar{V}|\,.\,\bar{V} \qquad (3.1)$$

where,

P = Pressure,

ϵ = Void fraction,

d_c= Diameter of the coke particles,

ρ_g= Density of gas,

$\bar{V}$ = Velocity,

D_f = Diameter of the furnace.

3.1.2.2 Steady-state equation:

Heat and mass transfer can be modeled according to the steady-state equation given below as [74],

$$D_e \frac{1}{r^2}\frac{\partial}{\partial r}\left(r^2 \frac{\partial \overline{C_A}}{\partial r}\right) - r_v \rho_p = \frac{\partial}{\partial \theta}\left(\varepsilon_p \overline{C_A}\right) \quad (3.2)$$

where,

r = Radius inside catalyst,

r_v= Overall reaction rate,

$\overline{C_A}$= Concentration of fluid reactant,

ρ_p= Density of the catalyst particle,

D_e= Diffusivity,

$\frac{\partial}{\partial \theta}\left(\varepsilon_p \overline{C_A}\right)$ = Transient term.

3.1.2.3 Reaction rate constant:

$$K = \frac{1-\epsilon}{\frac{1}{k_x E_f} + \frac{d_c}{6 k_f}} \quad (3.16)$$

where,

k_x= Mass transfer coefficient,

k_f= Rate constant,

E_f= Catalyst effectiveness factor.

The mass transfer coefficient (k_x) can be written as,

$$k_x = 2R_e^{-0.336}\,\bar{V} \quad (3.16\ a)$$

where,

R_e = Reynolds number.

The diameter (d_c) of the coke particle, diffusivity (D_e) and the mass transfer coefficient (k_x) can be related by Juttner modulus (φ) as,

$$\varphi = \sqrt{\frac{d_c^2\, k_x}{4\, D_e}} \quad (3.16\ b)$$

This helps to evaluate the catalyst effectiveness factor of equation 3.16 as,

$$E_f = \frac{3}{\varphi}\left\{\coth[\varphi] - \frac{1}{\varphi}\right\} \quad (3.16\ c)$$

Similarly, Rate constant (k_f) can be written as the temperature of the fluid as,

$$k_f = 6.25 \times 10^5 \exp\left(\frac{-22000}{T}\right) T^{0.5} \quad (3.16\ d)$$

where,

T = Temperature.

This concludes that the rate constant of the reactions depends on temperature, the velocity of fluid, mass transfer, and porosity.

3.1.2.4 Effective heat transfer coefficient:

$$h_O = \left(\frac{6(1-\epsilon)}{d_c}\right) h \quad (3.17)$$

where,

h_O = Effective heat transfer coefficient,

h = Heat transfer coefficient.

This helps to develop the heat transfer through convection easily.

The equation for calculating temperature can be derived from the heat transfer equation as,

$$\frac{\partial T}{\partial t} = -V_x \frac{\partial T}{\partial x} - V_y \frac{\partial T}{\partial y} + a\left(\frac{\partial^2 T}{\partial x^2} + \frac{\partial^2 T}{\partial y^2}\right) + \dot{Q} \quad (3.18)$$

where,

T = Temperature,

$\dot{Q}$= Heat generation term,

V= velocity,

a = Thermal conductivity,

x, y = x & y directions respectively.

This helps to develop an equation for the heat of generation of reacting species by using the assumption that the rate of product production is the same as the rate of reactant consumption. By using system boundary conditions of standard state we get,

$$\dot{Q}_{comb} + \dot{n}_c \bar{h}_c + \dot{n}_{O_2} \bar{h}_{O_2} - \dot{n}_{CO_2} \bar{h}_{CO_2} = 0 \quad (3.19)$$

where,

$\dot{Q}_{comb}$ = Heat generation by combustion,

$\dot{n}$= Molar flow rate,

$\bar{h}$ = Enthalpy of Formation.

Equation 3.19 can be reduced by deduction that CO_2 is the only heat-generating specie i.e. $\dot{n}_c = \dot{n}_{O_2} = \dot{n}_{CO_2}$

So,

$$\dot{Q}_{comb} = \dot{n}_{CO_2}(\bar{h}_{CO_2}) \tag{3.20}$$

And by calculating the number of moles of oxygen by multiplying reaction rate with the number of moles at present as [71],

$$KC_{O_2} = \dot{n}_{CO_2}$$

$$\dot{Q}_{comb} = \frac{1-\epsilon}{\frac{1}{k_x E_f}+\frac{d_c}{6k_f}}(\bar{h}_{CO_2})(C_{O_2}) \tag{3.21}$$

This helps to derive equations for the heat of gases and solids as,

$$\dot{Q}_g = \frac{1-\epsilon}{\frac{1}{k_x E_f}+\frac{d_c}{6k_f}}(\bar{h}_{CO_2})(\beta)(C_{O_2}) - h_0(T_g - T_O) \tag{3.22}$$

$$\dot{Q}_s = \frac{1-\epsilon}{\frac{1}{k_x E_f}+\frac{d_c}{6k_f}}(\bar{h}_{CO_2})(\beta)(C_{O_2}) - h_0(1-\alpha_{melt})(T_s - T_O) \tag{3.23}$$

where,

$\dot{Q}_g$ = Heat generation by gasses,

$\dot{Q}_s$ = Heat generation by solids,

α_{melt} = Melting factor,

β = Heat transferred to air from solids.

3.2.3 Modeling in MATLAB

3.2.3.1 Discretization

To calculate the value of heat, mass, energy, exergy, etc. inside the furnace, we need to divide the furnace into small units to calculate the values at each unit. This division of furnaces into small sections is known as Discretization of geometry. For example, if we create geometry by initializing the two variables for two-dimensional (2-D) geometry. For furnace geometry in 2-D, we need its Diameter and Height to be discretized.

```
%% Discretization %%
Diam=x;          % Diameter of the furnace ("x" cm)
H=y;             % Height of the furnace ("y" cm)
dx=z;            % Grid spacing ("z" cm)
m= Diam/dx+2;    % Discretization along Diameter
n= H/dx+2;       % Discretization along Height
```

This generates a matrix which is regarded as mesh in CFD of order n × m order with a grid spacing of z. This is shown in the figure below as well,

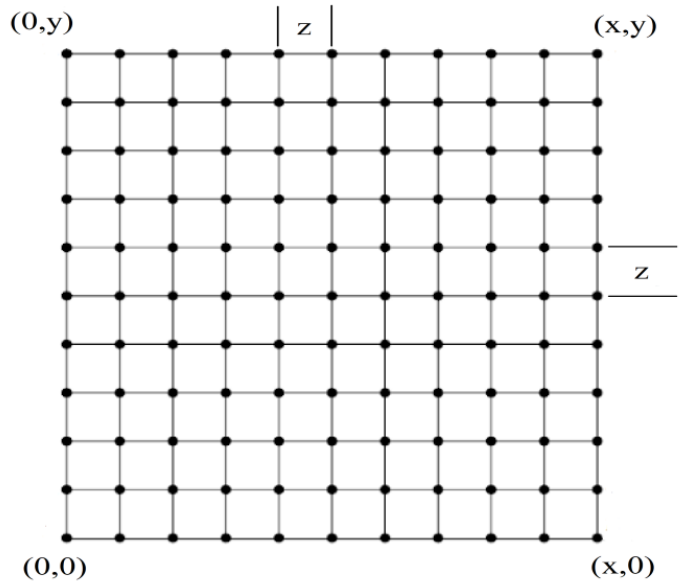

Figure 3.2: Grid Discretization

This discretization of the geometry creates a large matrix and hence, this matrix is used to calculate all the variables around.

3.2.3.2 Initialization of Parameters and Variables

It is highly recommended by the programmers to initialize matrices of all the variables and parameters as a dumpy zero matrix. This helps to reduce the convergence time for the program as it gets easy for the software to overwrite the values than re-initializing the matrix each time during the calculations within the loop. The MATLAB program calculates the value for each cell of the matrix so, we need to initialize the variable matrix of the same order i.e. for a grid of order n × m we need to generate separate matrices of order n × m. For example, for a dummy variable1, it can be initialized as,

```
%% Variables & Parameters initialization %%

Varible1=zeros(n,m);    % generates matrix of n×m with all zero values
```

Figure 3.3 illustrates the null matrix of order n × m.

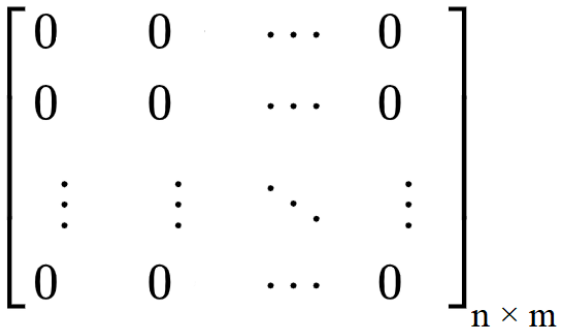

Figure 3.3: Null Matrix

3.2.3.3 Calculations in MATLAB

To calculate values on each cell of the matrix, the formula for a typical physical or chemical term remains the same but its input values depend upon the values of the surrounding. Hence, to repeat the calculation at each cell, we need to include some repetitive functions. These repetitive functions are known as loops in MATLAB. For calculating values within the geometry, two types of loops are used according to the requirement. These repetitive loops are discussed below,

- **While Loop**

  This type of repetitive statement helps to compare the answer with the preset value usually regarded as the allowable limit of the error. This loop keeps on working until the required statement becomes true or the value comes within the desired tolerance. This conditional looping is regarded as *error-checking* in MATLAB language [75]. For example, the pressure inside the furnace depends upon the velocity, vorticity, and initial boundary conditions of the components. So, while calculating the pressure values within the furnace we need to calculate the value by keeping in mind that the pressure value would decrease from the external pressure value. So, we define a dummy value to run and evaluate the function and then the *while loop* checks the value with the tolerance. If the value is within the range, it saves the value unless repeats the calculation with the new value which is calculated by the previous calculation hence near to the correct value but not the correct one. A typical error checking while loop is written as,

```
%% while loop for pressure error check %%

Pressure=1;                % Gives initial dummy value
count=0;           % Iteration Counting Variable
```

```
    %, while loop runs until value, gets less than 10^-6

While (pressure>1e-6);
       % calculates value according to the formula
        pressure=(pressure formula);
       % Counts the number of times while loop runs
        count=count+1;
end
```

- **Nested For Loop**

  For loop is regarded as an iterative loop as compared to conditional loop known as *while loops* [75]. *For loop* calculates the value for the range of cells of the matrix. For every equation discussed earlier, *for loop* is applied within the *while loop* remain within the acceptable range. A single *for loop* helps to evaluate the value in one dimension or generates values as a row vector. For each typical position along the x-axis, the furnace has an 'n' number of values along the height. So, to calculate all of them i.e. to add a dimension and making geometry 2-D it is required to another *for loop* within the first loop. This makes the program run for each cell of the 2-D matrix. This concept of '*for loop'* within the '*for loop'* is known as *"Nested for loop"*. When during the program run, the program enters first '*for loop'* within *'nested for loop'*; it runs for each value of the range given in the second *'for loop'*. When the program completes the range of the second loop, it exists this loop and the first loop in its way gets to the second iteration and again runs for all the values of the second *'for loop'*. This is illustrated in the figure below,

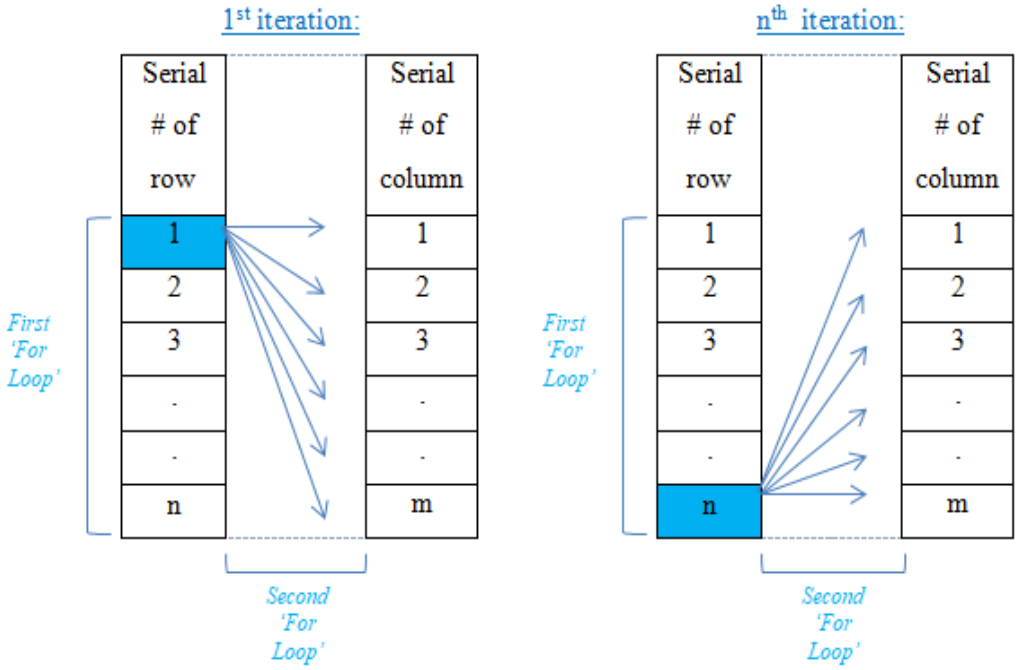

Figure 3.4: Nested For Loop Layout

In this work nested for loop is in a similar way. For example, equations 3.21, 3.22, and 3.23 can be rearranged to have temperature equation of solids and gases as,

For gasses,

$$T_{g(i,j)}^{n+1} = -u_{g(i,j)}\left(\frac{dt}{2dx}\right)\left(T_{g(i+1,j+1)}^{n} - T_{g(i-1,j)}^{n}\right) - v_{g(i,j)}\left(\frac{dt}{2dx}\right)\left(T_{g(i,j+1)}^{n} - T_{g(i,j-1)}^{n}\right) + \left(\frac{dt}{2dx}\right)\left(\frac{1}{Pe_g}\right)\left(T_{g(i+1,j)}^{n} - T_{g(i-1,j)}^{n}\right) + \left(T_{g(i,j-1)}^{n} - 4T_{g(i,j)}^{n}\right) + T_{g(i,j)}^{n} + Q_{g(i,j)} \quad (3.44\ a)$$

For solids,

$$T_{s(i,j)}^{n+1} = -u_{s(i,j)}\left(\frac{dt}{2dx}\right)\left(T_{s(i+1,j+1)}^{n} - T_{s(i-1,j)}^{n}\right) - v_{s(i,j)}\left(\frac{dt}{2dx}\right)\left(T_{s(i,j+1)}^{n} - T_{s(i,j-1)}^{n}\right) + \left(\frac{dt}{2dx}\right)\left(\frac{1}{Pe_s}\right)\left(T_{s(i+1,j)}^{n} - T_{s(i-1,j)}^{n}\right) + \left(T_{s(i,j-1)}^{n} - 4T_{s(i,j)}^{n}\right) + T_{s(i,j)}^{n} + Q_{s(i,j)} \quad (3.44\ b)$$

These two equations for temperature calculations are used in *nested for loop* to calculate the temperature at each cell of matric is shown below. Similar loops are used to calculate all the required variables in the study.

```
%% for loop for temperature %%
for i=1:n
    for j=1:m
    T_g(i,j)^(n+1) = -u_g(i,j)(dt/2dx)(T_g(i+1,j+1)^n - T_g(i-1,j)^n) - v_g(i,j)(dt/2dx)(T_g(i,j+1)^n - T_g(i,j-1)^n) + (dt/2dx)(1/Pe_g)(T_g(i+1,j)^n -
    T_g(i-1,j)^n) + (T_g(i,j-1)^n - 4T_g(i,j)^n) + T_g(i,j)^n + Q_g(i,j);   % equation 4.44 a for gas temp.
    T_s(i,j)^(n+1) = -u_s(i,j)(dt/2dx)(T_s(i+1,j+1)^n - T_s(i-1,j)^n) - v_s(i,j)(dt/2dx)(T_s(i,j+1)^n - T_s(i,j-1)^n) + (dt/2dx)(1/Pe_s)(T_s(i+1,j)^n -
    T_s(i-1,j)^n) + (T_s(i,j-1)^n - 4T_s(i,j)^n) + T_s(i,j)^n + Q_s(i,j);   % equation 4.44 b for solids temp.
    end
end
```

3.2.3.4 Exporting from MATLAB

The data obtained from the simulation is exported in three different ways which are described below;

- **Contour Plots**

  The velocity, concentration, energy, temperature, stream function and exergy data obtained as a function of height is displayed as contour plots. Contour plot actually assigns the colour code to the values in the MATLAB. These graphs easily explain the output and the readers understand the fluid flow and characteristics easily. The command of the contour plot used is given below,

```
%% Contour plots %%
% x & y represents matrix dimension; 'var' is a variable to be
plotted, 'n' is number of levels
contourf(x,y,variable,n,'linecolour',none)
% x (Diameter) and y (Height) axis ranges
axis([0 Diam 0 H]), daspect('auto')
% x and y labels, title and colour bar location respectively
xlabel(['x (units), Diameter: ', num2str(Diam)])
ylabel(['y (units), Height: ', num2str(H)])
title('variable')
colorbar('location','WestOutside')
```

- **Separate MATLAB data files**

  The data produced as output data files of MATLAB to be used later and reduce the iterative time. This helps to have initial variable output matrix as well in the next iteration and these files can be accessed separately if required, This follows a simple command as,

```
%% Exporting as MATLAB data %%
% Title=title of the file as desired; variable= variable to be saved in this
file
save(Title.mat','variable')
```

- **Excel Sheet**

  One of the major advantages of using MATLAB is that we can easily export the data in an excel sheet where it can be saved as a data set separately and can be used for post-processing by different soft wares. All the output data were exported to an Excel datasheet. Each time the simulation is converged, the data is exported automatically as a part of the code. The command used is as under,

```
%% Exporting to Excel worksheet %%
    % variable= any variable to be stored
filename = 'mydata.xlsx';
A = variable;
sheet = 1;
xlswrite(filename,A,sheet)
```

This MATLAB work can be summarized as a process flow diagram in figure 4.5 given below.

3.2.4 Application of ANN

The data set obtained by exporting the variable by using the functions discussed above was used to train and validate the ANN model. The variables data generated by the MATLAB model was used to apply the ANN model and predict the output for certain conditions. The primary objective of the performing ANN on the model is to predict output for the furnace and hence its efficient operation. While using ANN, the sigmoid transfer function is used to actuate the model variables output.

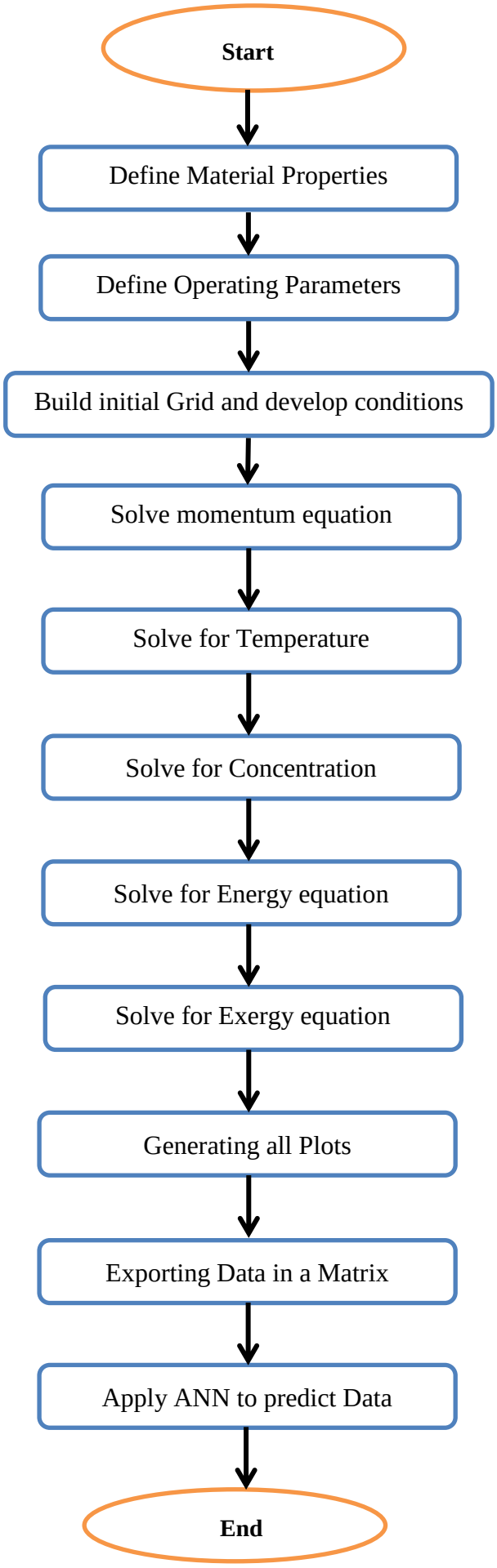

Figure 3.5: Model Development Schematic

Chapter 4

Results and Discussion

This section is divided into two parts. One describes in detail the modeling of the furnace in MATLAB. While second explains the Artificial Neural Network (ANN) results.

4.1 MATLAB Modeling Results and Validation

While modeling through MATLAB, different contour plots were obtained as results that were validated by two different sources. For air direction, the literature presenting the multi-component mathematical model of furnace is used. While the plots of temperature, oxygen concentration, velocity magnitude, and stream function obtained by simulation are validated by the research working for the same working parameters in another literature.

Based on these validated results, the kinetic, potential, and physical exergy of the furnace is calculated and presented.

4.1.1 Air Direction Profiles

The velocity vectors plotted from MATLAB using the velocity function described in the equations above show strong relation with the flow direction of air presented in the literature. CASTRO et al. [69] explained mathematically the flow direction of air within a typical blast furnace. The results obtained through MATLAB are represented in figure 4.1 (a) which reflects that air enters from the bottom inlets and flows the trace lines and leaves the furnace from the top. This helps to develop a base that all the reactions within the furnace are occurring efficiently. Oxygen is the base material for initiating reactions in the blast furnace as discussed above in detail. Due to oxygen further reactions with carbon monoxide works and reduces iron oxide into iron (the required product). So, by path tracing of oxygen it is much evident that oxygen is available enough for reaction within the furnace and the path lines correspond with literature with which it can be said that the parameters of the furnace under consideration are relatable with that of the actual furnace and hence, results are reliable.

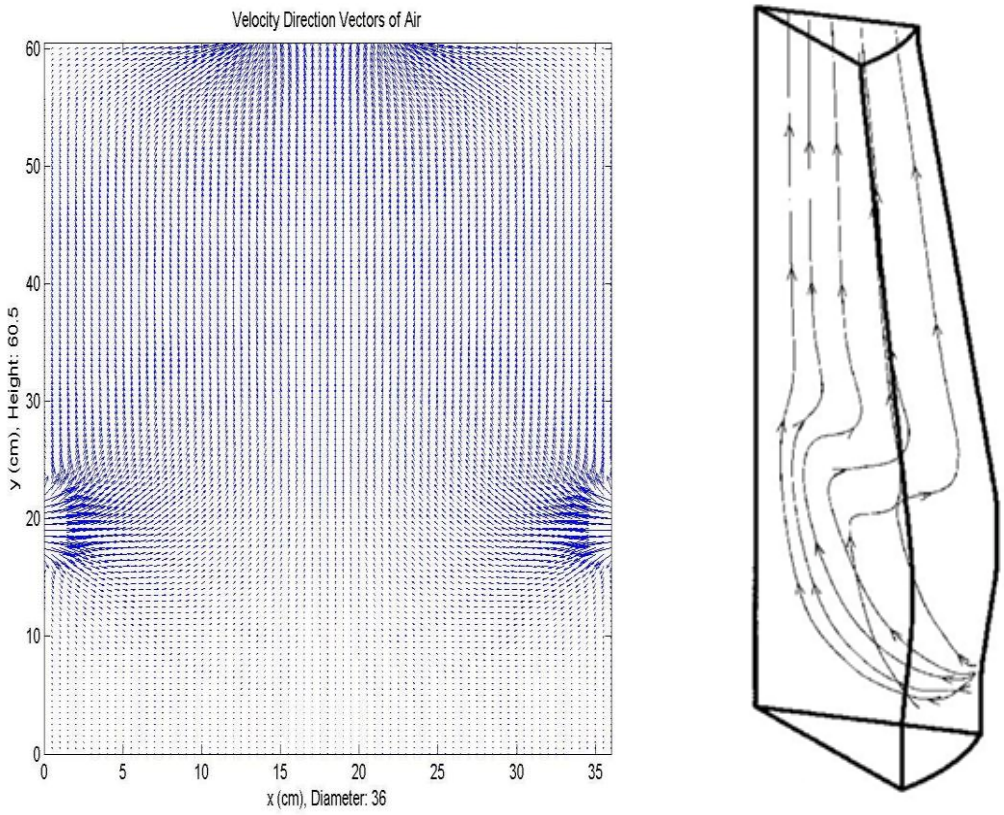

(a) (b)

Figure 4.1: Air profiles in the furnace results (a), literature (b) [69].

4.1.2 Oxygen Concentration

Oxygen concentration represents the presence of oxygen as alone. As air consists of 21 percent of oxygen and remaining is considered to be nitrogen. The air profiles reflect that oxygen along with nitrogen enters from the bottom inlets and move towards the top where it is extracted. While moving towards the top the air undergoes series of reactions which were discussed in detail in chapter 1. During these reactions, oxygen gets consumed to produce carbon monoxide which is further involved in iron oxide reduction reactions. Figure 4.2 (a) represents the results obtained while modeling in MATLAB. A similar technique with the same parameters is used by Kevin et al. [70]. He compares the results on the same dimensioned furnace with the same parameters obtained from MATLAB and ANSYS Fluent. The results obtained are found to be very much in confidence with his trends. This establishes the reliability of the model.

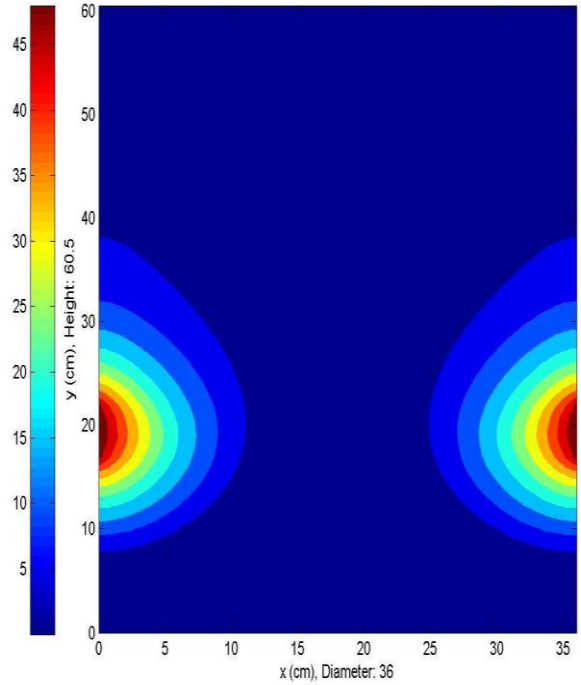

(a)

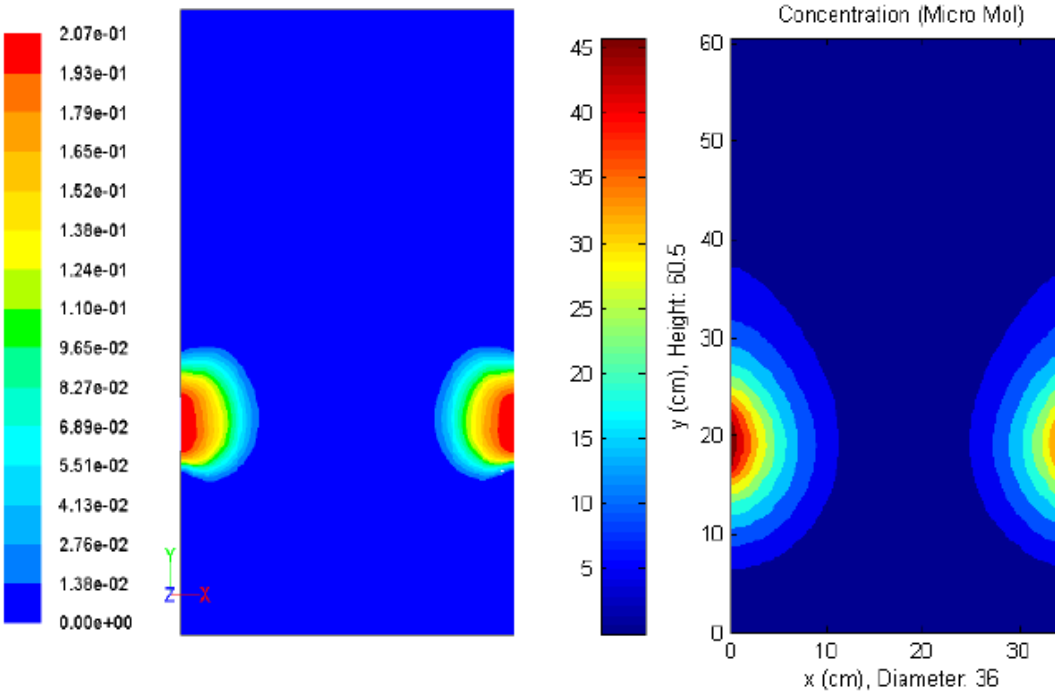

(b) (c)

Figure 4.2: Contours plots of Oxygen Concentration (a) Simulation Results (b) Literature Fluent results [70] (c) MATLAB Literature results [70]

4.1.3 Velocity Magnitude

As discussed earlier the parameters of the model were established according to the model presented by Kevin et al. [70]. To validate the model parameters, the velocity

magnitude in the furnace was generated as in the literature. The plot of velocity magnitude can also be compared with the graphs presented in the literature. In the furnace charge containing coke and iron ores with recycled iron is charged from the top while oxygen enters from the bottom. This makes velocity at the top i.e. the charge inlet and at the bottom i.e. the air inlet maximum. Within the furnace, this charge and air undergo series of reactions and iron keeps on moving downwards from where it is extracted. At the bottom, the molten iron is stored and a continuous flow is maintained. Hence, the velocity magnitude shows the same trend. This helps to validate the model parameters with the literature data as well.

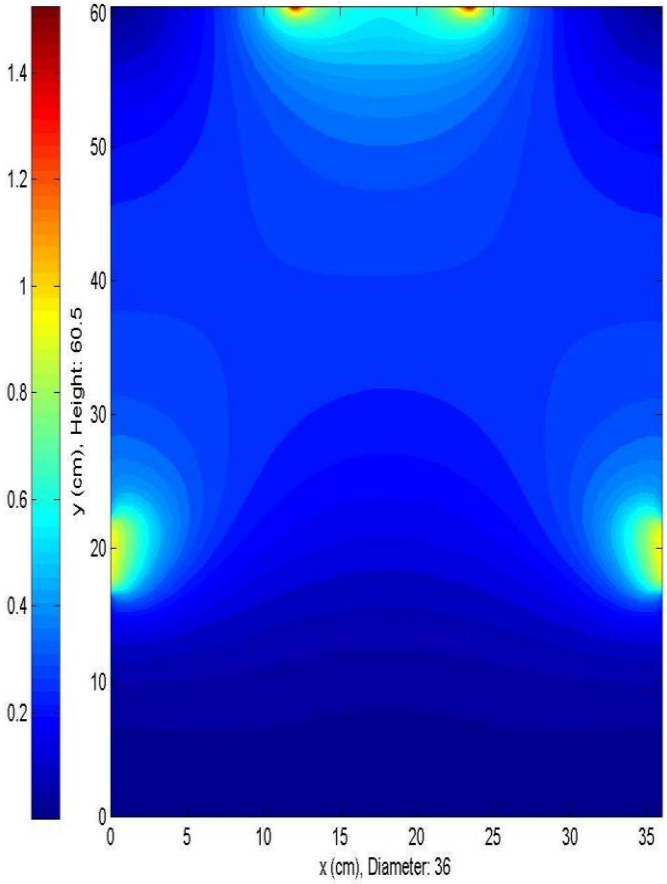

(a)

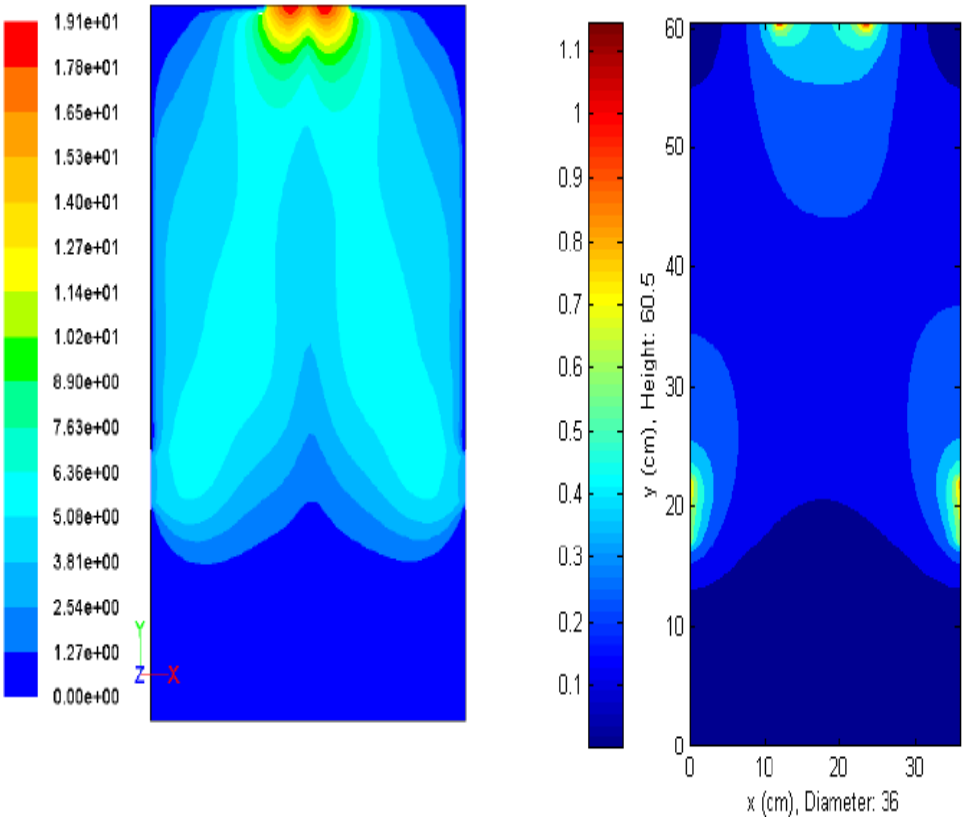

(b) (c)

Figure 4.3: Velocity Magnitude (a) simulation results (b) Literature Fluent results [70] (c) MATLAB Literature results [70]

4.1.4 Stream Function

Stream function represents the mass flow rate within the furnace. While writing the stream function formulae in MATLAB, the particle size of iron and void fraction is kept much smaller to have no difference from the literature under consideration. This makes the model vary a little from the fluent results presented in the literature. Moreover, the ANSYS Fluent variable defining enables the user to define the parameters like temperature-dependent pressure and density while in MATLAB for the sake of ease these parameters are kept constant. This makes the results a little different from the one presented in the literature for ANSYS Fluent in vertical streams. However, the maximum and minimum values of stream function are comparable and hence are considered to be validating the model.

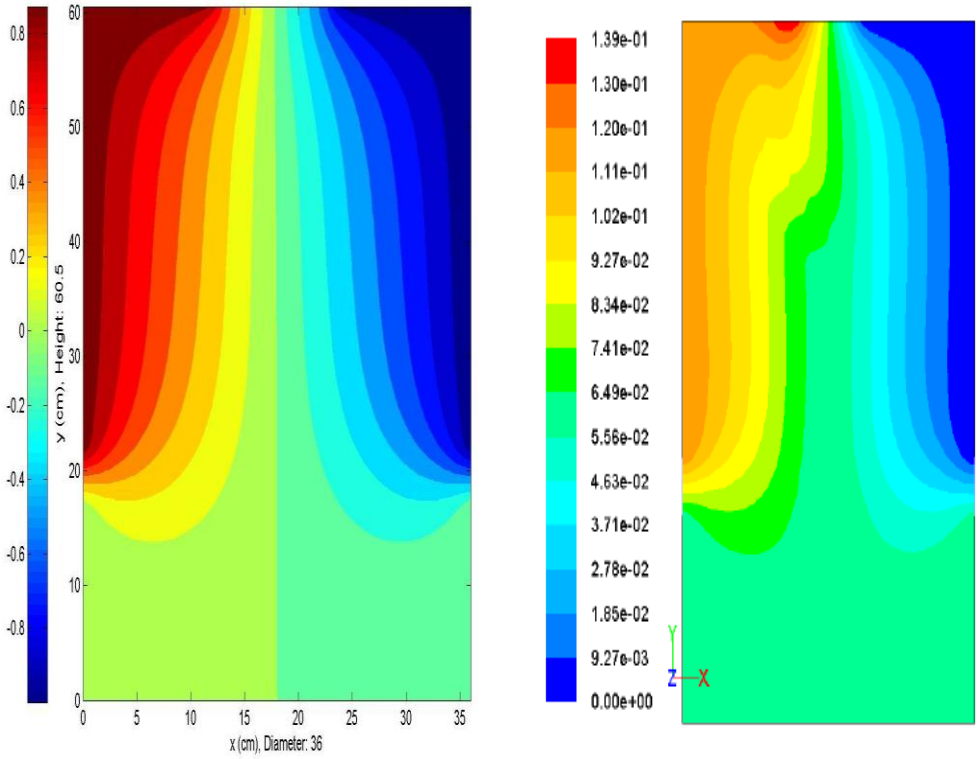

(a) (b)

Figure 4.4: Stream function (a) Simulation results (b) Literature Fluent results [70]

4.1.5 Temperature

Similarly, the case of temperature plots from the simulation in MATLAB and that of Fluent present in literature is found to be in good agreement. The results show that the temperature rises in the middle of the furnace as most of the reactions take place in the middle which makes the temperature rise in the middle. These results when compared with the reactions background given in chapter 1, it is evident that most of the energy is released during the reduction of iron with carbon monoxide. Hence, the air and charge entering the furnace at a particular temperature gets reacts in the middle and results in temperature rise. However, the little broadness in the temperature zones can again be justified by the fixed diameter of iron particles and temperature-independent density and pressure. This makes the gas in the furnace readily dissipate the heat and making the zones very much higher at temperature.

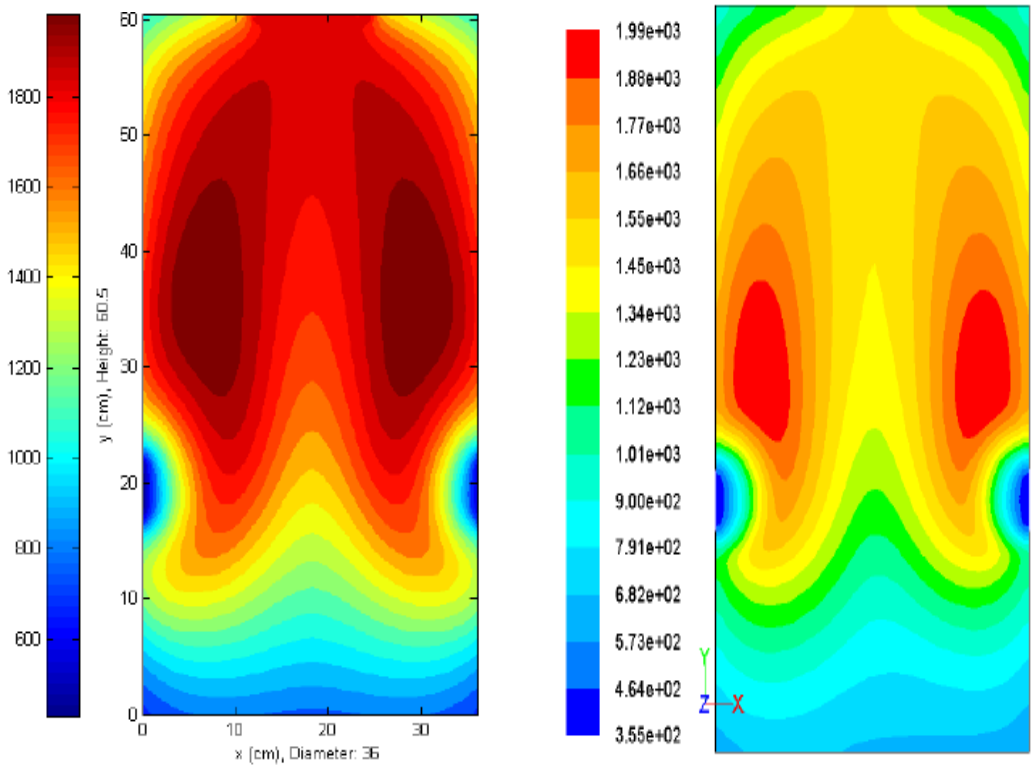

(a) (b)

Figure 4.5: Temperature (a) Simulation results (b) Literature Fluent results [70]

The temperature of the gas (i.e. air entering from the bottom) and the charge (i.e. coke and iron oxide entering from the top) enters the furnace at 298 kelvins. By moving towards the center, they experience a change in temperature due to the reaction. This trend for them is plotted separately in figure 4.5. This plot shows temperatures of charge and air at four different points along half of the diameter of the furnace. These results can be reflected in the center because the geometry is axisymmetric. Hence, near the wall temperature gets lower i.e. the red line and as we move towards the center temperature gets higher due to reactions is depicted by the green line in both cases. The little bump in the red line represents the sudden drop in the temperature due to the entrance of air at 298 kelvin at this level. This trend explains the temperature distribution within the furnace for the charge and the gas very well and helps to study the effect of inlet temperature of the charge and air on overall temperature as it is a part of the total temperature of the furnace at the particular position as well.

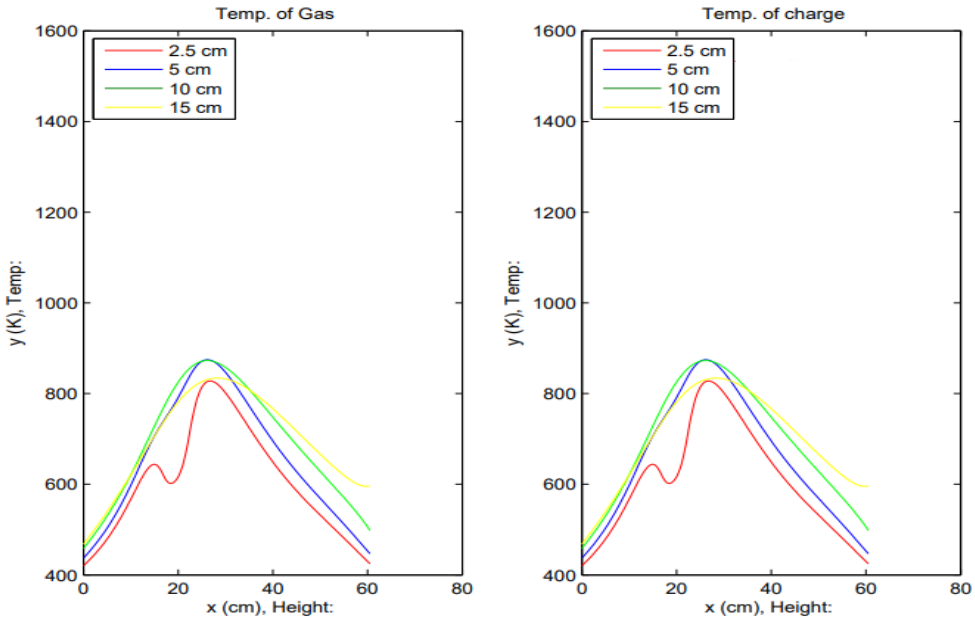

Figure 4.6: Temperature zones profiles by diameter along the height

4.1.6 Exergy

By validating the model with the results from the literature, it was found that the model developed via MATLAB using the process parameters as mentioned in the literature is reliable. Based on the validity of the model and the equations of the exergy discussed in Chapter 1, the exergy equations were similarly included in the code as temperature equations are discussed in section **3.2.3.3 nested for loops section.** Three types of exergy were calculated by this code-named potential, kinetic and physical exergy. The equations for all these exergies are comprised of three different equations. These equations form a separate matrix which was used to plot as a contour as shown in figure 4.5. These three exergies were summed up to display the total exergy of the furnace so far.

Figure 4.5 (b) represents the physical exergy of the furnace. According to equation 1.14, the physical exergy depends upon the temperature of the furnace the most. It can be observed that the furnace is found to be most exergetic at the points where the temperature profile of the furnace remains higher. Similarly, figure 4.5 (c) represents the kinetic exergy of the furnace. While observing equation 1.19, the kinetic exergy depends upon the product of the bulk velocity and the bulk flow rate at a typical position. This trend can be justified if the velocity magnitude in figure 4.3 (a) is observed. It is much evident that kinetic exergy is much higher at the point where

velocity is higher. The potential exergy of the furnace can be viewed in figure 4.5 (d). According to equation 1.20, it is the product of height altitude, mass flow rate, and velocity. Hence, velocity is the only factor which is having a higher effect on potential exergy and it is much higher in the high-velocity zones. While at other levels, it has the only effect of height altitude and mass flow rate which is minimized by the lower velocity levels at that position.

These three types of exergies are summed up to total exergy represented in figure 4.5 (a). The figure shows that most of the exergy is due to physical exergy while velocity magnitude is an important factor in potential and kinetic exergy; hence it makes values at top and entry levels of air in total exergy a little different from physical exergy.

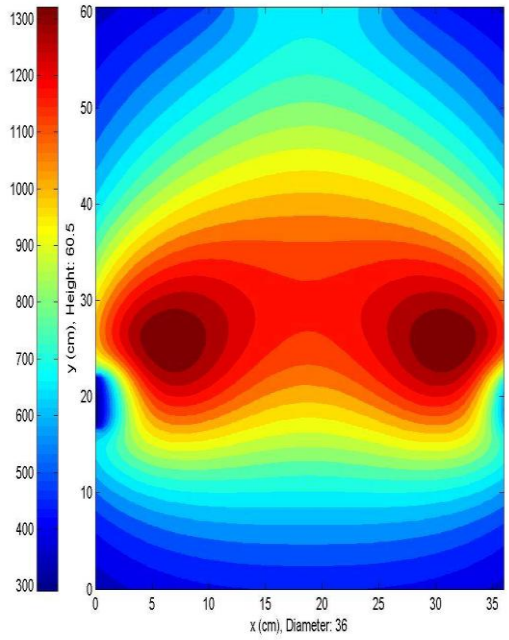

(a)

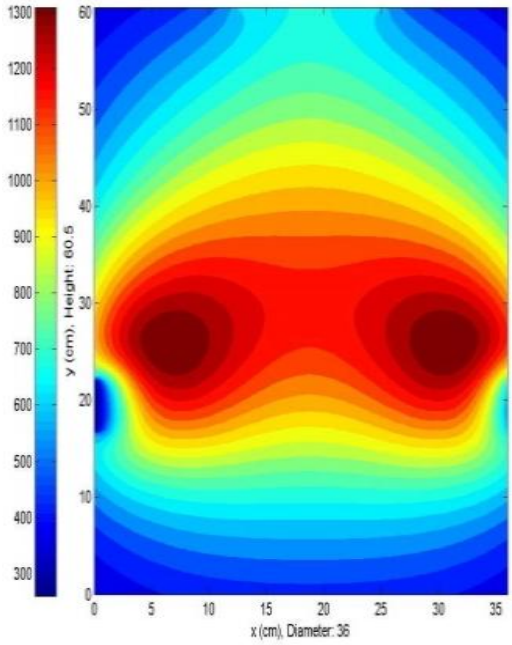

(b)

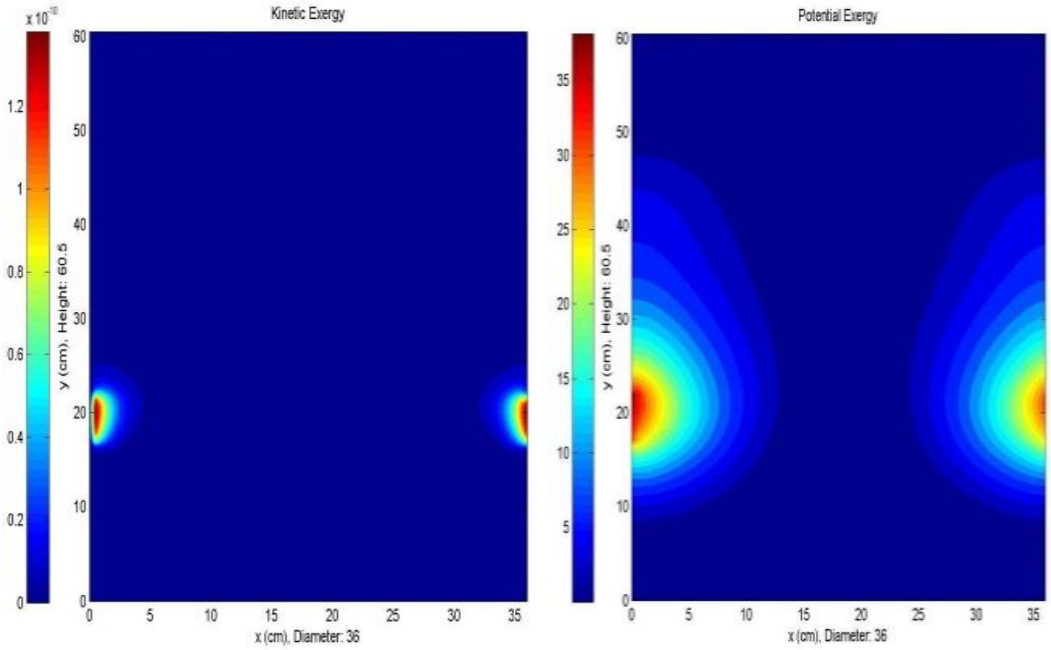

(c) (d)

Figure 4.7: Exergy Contours (a) Total Exergy (b) Physical Exergy (c) Kinetic Exergy (d) Potential Exergy

4.2 ANN model results

The ANN model used the data set obtained by the analysis done through MATLAB. The outputs of the furnace were predicted against the testing values and graphs were plotted against each other to compare the values. These predicted values were found to be very much in confidence with the training data as in all of them the value of *regression 'R'* is found to be very much near to unity. These plots are shown in figure 4.6.

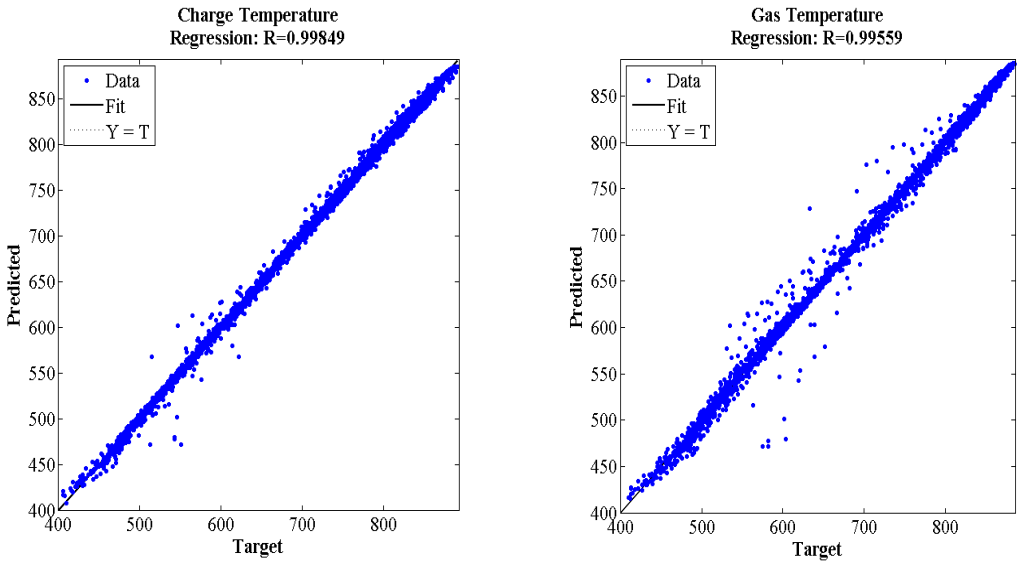

(a) (b)

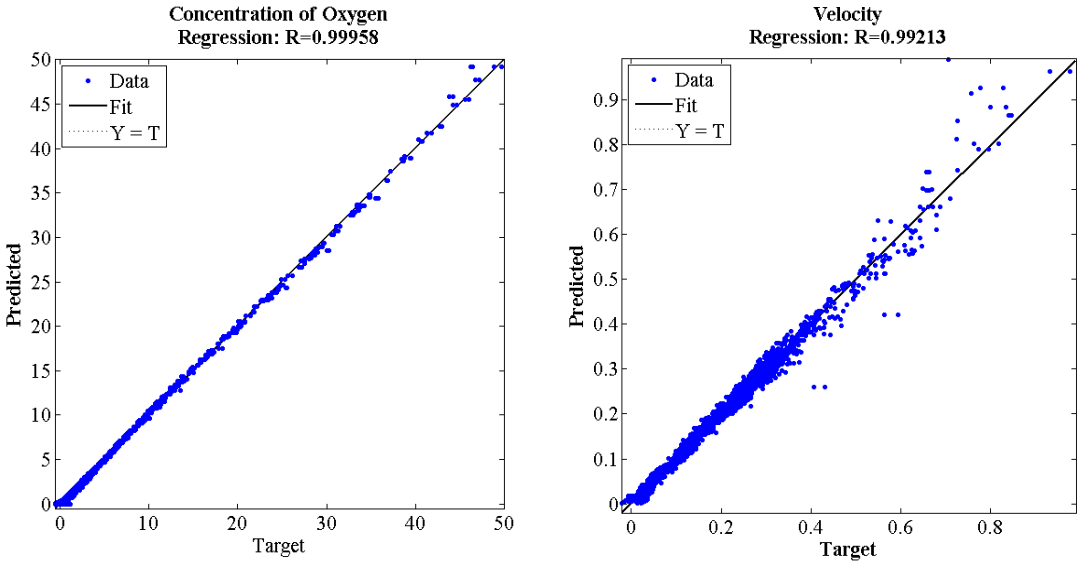

(c)

(d)

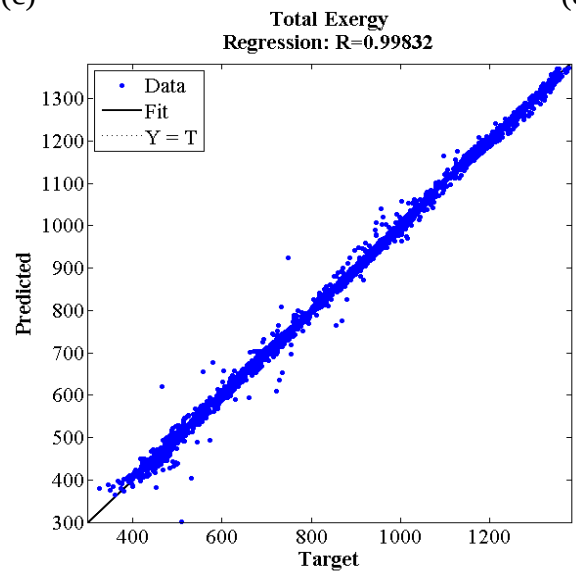

(e)

Figure 4.8: ANN regression plots (a) Charge temperature (b) Gas temperature (c) Concentration of Oxygen (d) Velocity (e) Total Exergy

It can be observed from figure 4.6, that the regression value for all the plots is very much accurate and hence the ANN model developed can be considered to be accurate, and hence the optimization and predictive analysis can be performed based upon the tool developed.

Conclusions and Recommendations

Conclusion

The simulation of Iron making furnace was done in MATLAB. The results were validated with the literature results from which the process parameters were adopted. Based on these results kinetic, potential, and physical exergy of the furnace was calculated and studied. The input and output data set of the furnace simulated earlier was used to develop the ANN-based predictive model as well. It was found that under the set parameters of the furnace, the furnace is 49 percent energy-efficient while the exergy efficiency of the furnace was found to be 28.5 percent. Hence, the model generated can be used to predict the exergy and energy efficiencies of the furnace under different conditions.

Recommendations

For future following recommendations can be made to have a productive work;

- Based on exergy calculations in this work, it is recommended to perform chemical and mixing exergy simulations as well.
- This work can also be a base for building the same bell-shaped geometry of the blast furnace as well. However, the task would involve some tedious equations but would be better.
- This work can also be made the base for 3-D modelling of furnace in MATLAB as well which would be using three for loops as nested loops.

References

[1] S. B. o. Pakistan, "Second Quarterly Report fiscal year 2016-Topical Section: Steel Sector: The Need for a Long Term Strategy," Report **2016**. [Online]. Available: http://221.120.204.42/reports/quarterly/fy16/Second/Topical.pdf

[2] W. Chen, X. Yin, and D. Ma, "A bottom-up analysis of China's iron and steel industrial energy consumption and CO2 emissions," *Applied Energy*, vol. 136, pp. 1174-1183, **2014**.

[3] A. Hasanbeigi, L. Price, Z. Chunxia, N. Aden, L. Xiuping, and S. Fangqin, "Comparison of iron and steel production energy use and energy intensity in China and the US," *Journal of cleaner production*, vol. 65, pp. 108-119, **2014**.

[4] J. Morfeldt and S. Silveira, "Capturing energy efficiency in European iron and steel production—comparing specific energy consumption and Malmquist productivity index," *Energy Efficiency*, vol. 7, no. 6, pp. 955-972, **2014**.

[5] N. Pardo and J. A. Moya, "Prospective scenarios on energy efficiency and CO2 emissions in the European Iron & Steel industry," *Energy*, vol. 54, pp. 113-128, **2013**.

[6] T. Xu, N. Karali, and J. Sathaye, "Undertaking high impact strategies: the role of national efficiency measures in long-term energy and emission reduction in steel making," *Applied energy*, vol. 122, pp. 179-188, **2014**.

[7] M. Geerdes, R. Chaigneau, and I. Kurunov, *Modern blast furnace ironmaking: an introduction (2015)*. Ios Press, **2015**.

[8] W. S. A. Economic Committee, Brussels, "Steel Statistical Yearbook **2012**," 2012**.** [Online]. Available: https://www.worldsteel.org/zh/dam/jcr:a0d5110b-80e1-4f1d-a6f0-a9054c07b672/Steel+Statistical+Yearbook+2012.pdf

[9] B. P. (BP). *BP Statistical Review of World Energy-Main Indicators*. [Online]. Available: https://knoema.com/BPWES2017/bp-statistical-review-of-world-energy-main-indicators?tsId=1005940

[10] G. o. P.-F. Department, "Pakistan Economic Survey (2016-17) -Overview," in "Overview," **2016-17**. [Online]. Available: http://www.finance.gov.pk/survey/chapters_17/overview_2016-17.pdf

[11] E. Generalic, "Croatian-English Chemistry Dictionary & Glossary," **2015**.

[12] S. S. Sun, "A study of kinetics and mechanisms of iron ore reduction in ore/coal composites," **1997**.

[13] R. H. Petrucci, F. G. Herring, C. Bissonnette, and J. D. Madura, *General chemistry: principles and modern applications*. Pearson, **2017**.

[14] S. Chastain, *Iron melting cupola furnaces for the small foundry*. Stephen Chastain, **2000**.

[15] J. Song, Z. Jiang, C. Bao, and A. Xu, "Comparison of energy consumption and CO2 emission for three steel production routes—Integrated steel plant equipped with blast furnace, oxygen blast furnace or COREX," *Metals,* vol. 9, no. 3, p. 364, **2019**.

[16] M. Harrington, "The reduction of magnetite and lean magnetite sinters," Sheffield Hallam University, **1972**.

[17] W. McKewan, "Kinetics of iron ore reduction," vol. 212, ed: MINERALS METALS MATERIALS SOC 420 COMMONWEALTH DR, WARRENDALE, PA 15086, **1958**, pp. 791-793.

[18] R. Spitzer, F. Manning, and W. Philbrook, "Mixed-control reaction kinetics in the gaseous reduction of hematite," *AIME MET SOC TRANS,* vol. 236, no. 5, pp. 726-742, **1966**.

[19] N. Sato, *Chemical energy and exergy: an introduction to chemical thermodynamics for engineers*. Elsevier, **2004**.

[20] N. R. Pal and S. K. Pal, "Object-background segmentation using new definitions of entropy," *IEE Proceedings E (Computers and Digital Techniques),* vol. 136, no. 4, pp. 284-295, **1989**.

[21] J. Szargut, *Exergy method: technical and ecological applications*. WIT press, **2005**.

[22] T. J. Kotas, *The exergy method of thermal plant analysis*. Elsevier, **2013**.

[23] G. Tsatsaronis, "Definitions and nomenclature in exergy analysis and exergoeconomics," *Energy,* vol. 32, no. 4, pp. 249-253, **2007**.

[24] T. Morosuk and G. Tsatsaronis, "Splitting physical exergy: Theory and application," *Energy,* vol. 167, pp. 698-707, **2019**.

[25] J. Mustafa, I. Ahmad, M. Ahsan, and M. Kano, "Computational fluid dynamics based model development and exergy analysis of naphtha reforming reactors," *International Journal of Exergy,* vol. 24, no. 2-4, pp. 344-363, **2017**.

[26] J. S. Almeida and P. A. Noble, "Neural computing in microbiology," ed: Elsevier, **2000**.

[27] H.-Y. Kang, R. Rule, and P. Noble, "Artificial neural network modeling of phytoplankton blooms and its application to sampling sites within the same estuary," **2011**.

[28] I. A. Basheer and M. J. J. o. m. m. Hajmeer, "Artificial neural networks: fundamentals, computing, design, and application," vol. 43, no. 1, pp. 3-31, **2000**.

[29] D. Fu, Y. Chen, and C. Q. J. A. M. M. Zhou, "Mathematical modeling of blast furnace burden distribution with non-uniform descending speed," vol. 39, no. 23-24, pp. 7554-7567, **2015**.

[30] A. Dmitriev, *Mathematical Modeling of the Blast Furnace Process*. Cambridge Scholars Publishing, **2019.**

[31] P. Jin, Z. Jiang, C. Bao, Y. Lu, J. Zhang, and X. J. s. r. i. Zhang, "Mathematical modeling of the energy consumption and carbon emission for the oxygen blast furnace with top gas recycling," vol. 87, no. 3, pp. 320-329, **2016**.

[32] W. Sun, Z. Wang, and Q. J. E. Wang, "Hybrid event-, mechanism-and data-driven prediction of blast furnace gas generation," p. 117497, **2020**.

[33] B. K. Mahanta and N. J. s. r. i. Chakraborti, "Evolutionary data driven modeling and multi objective optimization of noisy data set in blast furnace iron making process," vol. 89, no. 9, p. 1800121, **2018**.

[34] P. Zhou, H. Song, H. Wang, and T. J. I. T. o. C. S. T. Chai, "Data-driven nonlinear subspace modeling for prediction and control of molten iron quality indices in blast furnace ironmaking," vol. 25, no. 5, pp. 1761-1774, **2016**.

[35] M. Yuan *et al.*, "Intelligent multivariable modeling of blast furnace molten iron quality based on dynamic AGA-ANN and PCA," vol. 22, no. 6, pp. 487-495, **2015**.

[36] R. Acosta-Herazo, B. Cañaveral-Velásquez, K. Pérez-Giraldo, M. A. Mueses, M. H. Pinzón-Cárdenas, and F. J. W. Machuca-Martínez, "A MATLAB-Based Application for Modeling and Simulation of Solar Slurry Photocatalytic Reactors for Environmental Applications," vol. 12, no. 8, p. 2196, **2020**.

[37] T. M. Ismail, K. Ramzy, B. E. Elnaghi, M. Abelwhab, M. J. E. C. Abd El-Salam, and Management, "Using MATLAB to model and simulate a photovoltaic system to produce hydrogen," vol. 185, pp. 101-129, **2019**.

[38] L. Prades, A. Dorado, J. Climent, X. Guimerà, S. Chiva, and X. J. C. E. J. Gamisans, "CFD modeling of a fixed-bed biofilm reactor coupling hydrodynamics and biokinetics," vol. 313, pp. 680-692, **2017**.

[39] F. Logist, P. Saucez, J. Van Impe, and A. V. J. C. E. J. Wouwer, "Simulation of (bio) chemical processes with distributed parameters using Matlab®," vol. 155, no. 3, pp. 603-616, **2009**.

[40] C. Spiegel, *PEM fuel cell modeling and simulation using MATLAB*. Elsevier, **2011**.

[41] R. Molina, G. Orcajo, and F. J. E. f. C. E. Martinez, "KBR (Kinetics in Batch Reactors): a MATLAB-based application with a friendly Graphical User Interface for chemical kinetic model simulation and parameter estimation," vol. 28, pp. 80-89, **2019**.

[42] I. Dincer, T. J. W. I. R. E. Ratlamwala, and Environment, "Importance of exergy for analysis, improvement, design, and assessment," vol. 2, no. 3, pp. 335-349, **2013**.

[43] W. Zhang, J. Zhang, and Z. J. E. Xue, "Exergy analyses of the oxygen blast furnace with top gas recycling process," vol. 121, pp. 135-146, **2017**.

[44] T. L. Guo, M. S. Chu, Z. G. Liu, J. Tang, and J. I. J. s. r. i. Yagi, "Mathematical modeling and exergy analysis of blast furnace operation with natural gas injection," vol. 84, no. 4, pp. 333-343, **2013**.

[45] A. Ziębik and W. J. I. j. o. e. r. Stanek, "Influence of blast- furnace process thermal parameters on energy and exergy characteristics and exergy losses," vol. 30, no. 4, pp. 203-219, **2006**.

[46] T. Suetens, B. Klaasen, K. Van Acker, and B. J. J. o. c. p. Blanpain, "Comparison of electric arc furnace dust treatment technologies using exergy efficiency," vol. 65, pp. 152-167, **2014**.

[47] M. Børset, L. Kolbeinsen, H. Tveit, and S. J. E. Kjelstrup, "Exergy based efficiency indicators for the silicon furnace," vol. 90, pp. 1916-1921, **2015**.

[48] M. Hasanuzzaman, R. Saidur, and N. J. I. J. o. P. S. Rahim, "Energy, exergy and economic analysis of an annealing furnace," vol. 6, no. 6, pp. 1257-1266, **2011**.

[49] Ü. Çamdali and M. J. A. T. E. Tunç, "Exergy analysis and efficiency in an industrial AC electric ARC furnace," vol. 23, no. 17, pp. 2255-2267, **2003**.

[50] F. Calise, M. D. d'Accadia, A. Palombo, and L. J. E. Vanoli, "Simulation and exergy analysis of a hybrid solid oxide fuel cell (SOFC)–gas turbine system," vol. 31, no. 15, pp. 3278-3299, **2006**.

[51] M. E. Yousef Nezhad, S. J. J. o. R. Hoseinzadeh, and S. Energy, "Mathematical modelling and simulation of a solar water heater for an aviculture unit using MATLAB/SIMULINK," vol. 9, no. 6, p. 063702, **2017**.

[52] E. S. Dogbe, M. A. Mandegari, and J. F. J. E. Görgens, "Exergetic diagnosis and performance analysis of a typical sugar mill based on Aspen Plus® simulation of the process," vol. 145, pp. 614-625, **2018**.

[53] P. Ahmadi, I. Dincer, and M. A. J. I. J. o. H. E. Rosen, "Energy and exergy analyses of hydrogen production via solar-boosted ocean thermal energy conversion and PEM electrolysis," vol. 38, no. 4, pp. 1795-1805, **2013**.

[54] B. Ghorbani, Z. Javadi, S. Zendehboudi, M. J. E. C. Amidpour, and Management, "Energy, exergy, and economic analyses of a new integrated system for generation of power and liquid fuels using liquefied natural gas regasification and solar collectors," vol. 219, p. 112915, **2020**.

[55] J. M. Montelongo- Luna, W. Y. Svrcek, and B. R. Young, "The relative exergy array—a new measure for interactions in process design and control," *The Canadian Journal of Chemical Engineering*, vol. 89, no. 3, pp. 545-549, **2011**.

[56] M. Munir, W. Yu, and B. Young, "The relative exergy- destroyed array: A new tool for control structure design," *The Canadian Journal of Chemical Engineering*, vol. 91, no. 10, pp. 1686-1694, **2013**.

[57] E. Querol, B. Gonzalez-Regueral, and J. L. Perez-Benedito, *Practical approach to exergy and thermoeconomic analyses of industrial processes*. Springer Science & Business Media, **2012**.

[58] A. Hinderink, F. Kerkhof, A. Lie, J. D. S. Arons, and H. Van Der Kooi, "Exergy analysis with a flowsheeting simulator—I. Theory; calculating exergies of material streams," *Chemical Engineering Science*, vol. 51, no. 20, pp. 4693-4700, **1996**.

[59] X. Huang *et al.*, "Exergy distribution characteristics of solar-thermal dissociation of NiFe2O4 in a solar reactor," *Energy,* vol. 123, pp. 131-138, **2017**.

[60] M. Farmahini–Farahani, "Investigation of four geometrical parameters on thermal stratification of cold water tanks by exergy analysis," *International Journal of Exergy,* vol. 10, no. 3, pp. 332-345, **2012**.

[61] A. Yong-an, G. Xing-quan, S. Lin, W. Yue-ren, and F. Guo-hui, "Exergy analysis of exhaust-gas of burning liquefied-gas in a Chinese kitchen," in *2009 International Conference on Energy and Environment Technology*, **2009**, vol. 3: IEEE, pp. 40-43.

[62] S. K. J. J. T. I. o. E. Bag, "ANN based prediction of blast furnace parameters," vol. 68, no. 1, pp. 37-42, **2007**.

[63] S. Golestani and H. J. I. T. o. E. E. S. Samet, "Polynomial- dynamic electric arc furnace model combined with ANN," vol. 28, no. 7, p. e2561, **2018**.

[64] C. Bilim, C. D. Atiş, H. Tanyildizi, and O. J. A. i. E. S. Karahan, "Predicting the compressive strength of ground granulated blast furnace slag concrete using artificial neural network," vol. 40, no. 5, pp. 334-340, **2009**.

[65] J. G. Peacey and W. G. Davenport, *The iron blast furnace: theory and practice*. Elsevier, **2016**.

[66] U. n. C¸ amdali and M. J. J. E. R. T. Tunc¸, "Computation of chemical exergy potential in an industrial AC electric ARC furnace," vol. 127, no. 1, pp. 66-70, **2005**.

[67] T. Mahlia, B. Taufiq, K. Ong, R. J. E. Saidur, and Buildings, "Exergy analysis for day lighting, electric lighting and space cooling systems for a room space in a tropical climate," vol. 43, no. 7, pp. 1676-1684, **2011**.

[68] Q. Qin, X. Zhang, S. Lv, Q. Yu, and D. Lang, "Exergy Analysis of Ironmaking System," in *2012 Asia-Pacific Power and Energy Engineering Conference*, **2012**: IEEE, pp. 1-4.

[69] J. A. de CASTRO, H. Nogami, and J.-i. J. I. i. Yagi, "Three-dimensional multiphase mathematical modeling of the blast furnace based on the multifluid model," vol. 42, no. 1, pp. 44-52, **2002**.

[70] K. Dartt, *Computational Modeling and Optimization of an Iron Melting Cupollette Furnace*. State University of New York at Binghamton, Thomas J. Watson School of …, **2011**.

[71] N. Viswanathan, M. N. Srinivasan, and A. K. J. I. i. Lahiri, "Process simulation of cupola," vol. 38, no. 10, pp. 1062-1068, **1998**.

[72] N. Viswanathan, M. N. Srinivasan, A. K. J. I. Lahiri, and Steelmaking, "Steady state three-dimensional mathematical model for cupola," vol. 24, no. 6, pp. 476-483, **1997**.

[73] R. S. J. U. h. w. p. c. f.-t.-p.-b.-f.-b.-c.-u.-e. h. Subramanian, "Flow through packed beds and fluidized beds," **2004**.

[74] N. Wakao and S. Kagei, *Heat and mass transfer in packed beds*. Taylor & Francis, **1982**.

[75] S. Attaway, *Matlab: a practical introduction to programming and problem solving*. Butterworth-Heinemann, **2013**.